ELECTRIC AND MAGNETIC PROPERTIES OF HF, HCl, AND OCS BY MBER-SPECTROSCOPY

F. H. DE LEEUW

ELECTRIC AND MAGNETIC PROPERTIES OF HF, HCl, AND OCS BY MBER-SPECTROSCOPY

PROMOTOR: PROF. DR. A. DYMANUS

ELECTRIC AND MAGNETIC PROPERTIES OF HF, HCl, AND OCS BY MBER-SPECTROSCOPY

PROEFSCHRIFT

TER VERKRIJGING VAN DE GRAAD VAN DOCTOR
IN DE WISKUNDE EN NATUURWETENSCHAPPEN AAN DE
KATHOLIEKE UNIVERSITEIT TE NIJMEGEN, OP GEZAG VAN
DE RECTOR MAGNIFICUS DR. G. BRENNINKMEIJER,
HOOGLERAAR IN DE FACULTEIT DER SOCIALE WETENSCHAPPEN,
VOLGENS BESLUIT VAN DE SENAAT IN HET OPENBAAR TE
VERDEDIGEN OP VRIJDAG 25 JUNI 1971
DES NAMIDDAGS TE 2.00 UUR PRECIES

DOOR

FRANCISCUS HERMANUS DE LEEUW

geboren te Nijmegen

1971
DRUKKERIJ GEBR. JANSSEN N.V. NIJMEGEN

De velen, die op enigerlei wijze bijgedragen hebben in het tot stand komen van dit proefschrift wil ik hier gaarne bedanken. Enkelen van hen wil ik in het bijzonder vermelden.

Dr. R. van Wachem, die medegewerkt heeft in de aanvangsperiode van het onderzoek.

De heer L. Hendriks, die veel geholpen heeft bij het opbouwen van de apparatuur.

Dr. J. Reuss, die te allen tijde klaar stond om over mijn problemen te diskussiëren.

Diegenen, die tijdens hun afstudeerperiode stage gelopen hebben bij dit onderzoek en daarmee wezenlijke bijdragen geleverd hebben tot het tot stand komen er van.

De leden van de Werkgroep Atoom- en Molekuulfysika voor hun prettige samenwerking.

De heren W. van Royen en J. W. Elich voor hun hulp bij het ontwerpen van de meeste onderdelen van de apparatuur.

De dienstverlenende afdelingen wil ik gaarne bedanken in de personen van de heren J. G. M. van Langen en Ir. H. C. den Daas.

De illustratie afdeling onder de leiding van de heer J. Gerritsen voor het verzorgen van de illustraties in dit proefschrift.

Dr. O. B. Dabbousi and Dr. H. L. Schwartz for their help in preparing the manuscript.

Deze dankbetuiging zou niet volledig zijn als mijn vrouw niet genoemd werd voor o.a. het vele typewerk.

Voor mijn ouders
Voor Wiesje en
Marie-Louise, Jacqueline,
Margriet, Liesbeth en Frans

CONTENTS

CHAPTER I

INTRODUCTION

I.1 INTRODUCTION

A good knowledge of electric and magnetic properties of molecules is desired as they play an important role in transport processes and molecular interactions. These properties have been extensively investigated by various experimental and theoretical methods. Most theoretical investigations have been performed on simple molecules, as only these molecules are accessible to accurate ab-initio calculations. The hydrogen molecule and the first- and second-row diatomic hydrides are examples of such simple systems. Experimental results not only supply new information, but may serve, too, as a test of the theoretical calculations.

The electric and magnetic properties of the hydrogen molecule, a prototype of a two electron molecular system, have been thoroughly investigated. The experiments of Ramsey and his collaborators (Ram 40, Bar 54, Qui 58), performed with the molecular-beam magnetic-resonance (MBMR) method, have provided the values of various of these properties for three isotopic species of the hydrogen molecule (H_2, D_2 and HD) in two rotational states. The direct results of these experiments were the nuclear hyperfine properties, the rotational magnetic dipole moment, and the anisotropy in the magnetic susceptibility. It was shown by Ramsey (Ram 50) that the electric quadrupole moment of a molecule and the anisotropy in the diamagnetic susceptibility can be evaluated from the latter two quantities. The MBMR experiments on the hydrogen molecule have shown that this method provides an excellent capability for determining these quantities very accurately. Recently, an ab-initio calculation of the molecular quadrupole moment of the hydrogen molecule has been reported by Wołniewicz (Woł 66). The effects of the molecular vibration and rotation were taken into account in this calculation. Good agreement was found with the experimental result from the MBMR method.

Accurate measurements by the molecular-beam electric-resonance (MBER) method have been performed recently on the molecules HF (Mue 70) and HCl (Kai 70). The direct results of these experiments were the electric dipole moments and the nuclear hyperfine properties of these molecules. Isotopic and vibrational effects, which were neglected in previous investigations, were included in the latter measurements. The rotational magnetic dipole moment of the HF molecule was measured previously by Baker (Bak 61) using the MBMR

method, but the remaining magnetic properties had not been experimentally investigated until now.

This thesis reports the investigation of electric as well as magnetic properties of the HF and HCl molecules by the molecular-beam electric-resonance method. The observed properties are: the nuclear hyperfine properties, the molecular electric and magnetic dipole moments, the anisotropies in the magnetic susceptibility and the anisotropies in the nuclear magnetic shielding. The average magnetic shielding of the chlorine nucleus in HCl has also been obtained. The molecular quadrupole moment and the anisotropy in the diamagnetic susceptibility of HF and HCl are calculated from the present results using the relation derived by Ramsey (Ram 50). Using an analogous relationship (Ram 51), the anisotropy in the diamagnetic shielding is calculated from the magnetic shielding anisotropy and a certain nuclear hyperfine property (Chap. 5). The latter anisotropy was not observed in the hydrogen experiments. An observation of the susceptibility and shielding effects in HF was beyond the resolving power of the apparatus used by Baker (Bak 61). The anisotropy in the diamagnetic susceptibility and the molecular quadrupole moment of HF and HCl are determined in this work to within a few per cent.

The ab-initio calculations on HF and HCl which have been performed in the past four years (Cad 67a, Cad 67b, McL 67, Ben 69, Rot 70) show a increasing complexity, but give also more accurate predictions for properties such as electric dipole moments (Ben 69). The present experimental results may serve as a test of these calculations, showing whether the quantities, obtained in this work, can also be accurately calculated.

The molecular quadrupole moments of HF and HCl were obtained previously from line broadening experiments by Benedict and Herman (Ben 63). Line broadening experiments on H_2 (Ber 66) have shown, however, that these data are less reliable than molecular beam data. The reason for this is that the line broadening theories are as yet not well developed (Ber 66). The evaluation of the molecular quadrupole moment from the magnetic susceptibility anisotropy, however, is straightforward. The good agreement between the observed and calculated quadrupole moment of the hydrogen molecule is evidence of this. A comparison of the line broadening data of HF and HCl with the molecular beam data is therefore interesting.

The anisotropies in the diamagnetic shielding of the hydrogen nuclei in HF and HCl are accurately determined. The anisotropy in the diamagnetic shielding of the halogen nuclei was found equal to zero within the stated error limits. Until now the shielding anisotropy was only observed in the alkali fluorides (Dre 61, Grä 63, Grä 67, and references therein). These molecules are, however, not well accessible to theoretical calculations. Probably because of the scarce

experimental information, this quantity has only been calculated once up to now.

Measurements on three isotopic species of the OCS molecule ($^{16}O^{12}C^{32}S$, $^{16}O^{12}C^{34}S$, and $^{16}O^{13}C^{32}S$) are included in this work to test the performance of the apparatus. The results are also used to clear up some ambiguities which exist concerning the electric dipole moment and the molecular quadrupole moment of this molecule. The ambiguity concerning the molecular quadrupole moment originates from differing results for this quantity obtained from various line-broadening theories and experiments (Ber 66, Mur 68) and from measurements of magnetic susceptibility anisotropy using microwave Zeeman spectroscopy (Taf 68, Fly 69). The electric dipole moment determination was undertaken to check the measurement performed by Muenter (Mue 68) from which it was concluded that an older measurement performed by Marshall and Weber (Mar 57) was wrong. This was particularly serious as Marshall and Webers value was used as a standard for electric dipole moment measurements. We have confirmed the result obtained by Muenter (Mue 68), and the greater precision of our result may provide an accurate standard for electric dipole moments. The measurements on the isotopic species are also used to obtain the sign of the electric dipole moment of OCS and serve further as a critical test of the determination of molecular quadrupole moments from susceptibility anisotropy measurements as the molecular quadrupole moments for the different isotopic species are obtained in different coordinate systems. The measurements on $^{16}O^{13}C^{32}S$ have provided the shielding properties of the ^{13}C in OCS. The results can be compared with calculated results for CO and CH_2O.

The basis design features of the present molecular beam apparatus are similar to the designs of Drechsler and Gräff (Dre 61), Weiss (Wei 63), and of Van Wachem (Wac 67). However, advances in vacuum and other technologies have enabled us to construct a universal apparatus which combines all features of previous designs. The spectrometer is equipped with an electromagnet producing a homogeneous field in a rather long resonance region, with quadrupole fields which can sustain high field strengths to study molecules and molecular states with a weak Stark effect, and with a universal molecular beam detector housed in an ultrahigh vacuum system. These features make it possible to accurately investigate electric as well as magnetic properties, at least in principle, of any molecule.

I.2 SPECTROSCOPIC METHODS FOR THE DETERMINATION OF MAGNETIC PROPERTIES OF MOLECULES

This section is devoted to a discussion of spectroscopic methods which are in use at this time to determine magnetic properties of molecules such as the

magnetic susceptibility anisotropy and nuclear shielding anisotropy. A discussion of the nmr technique which makes possible the determination of the average value of the nuclear shielding is outside the scope of this work.

The energy levels of a closed shell ($^1\Sigma$) molecule will be split and shifted when it is subjected to an external magnetic field. The displacements of the energy levels depend on the strength of the field and on the magnitude of the molecular magnetic dipole moment, the molecular magnetic susceptibility, the nuclear moment(s), and the nuclear shielding. The smallest contribution to the energy of the molecule are due to the susceptibility and shielding effects. At a field of about 10 kG, which is normally obtainable with laboratory magnets, the displacements of the energy levels of the HF and HCl molecules due to the susceptibility and shielding effects are of the order of 1 kHz.[1] The latter effects can therefore only be evaluated from measurements in very strong magnetic fields or with a spectrometer which offers high resolution.[2]

The displacements of the energy levels due to the magnetic susceptibility of the molecule are proportional to the square of the magnetic field strength (Chap. 3). At very high magnetic fields it is possible to evaluate the susceptibility effects from microwave rotational spectra, as the half-widths [2] of the spectral lines observed with a conventional microwave spectrometer operating at a sufficiently low pressure are of the order of 25 kHz. These half-widths are determined by the broadening of the lines due to the Doppler effect. Flygare and collaborators (Fly 69, Fly 71) have measured the magnetic susceptibility anisotropies and the molecular quadrupole moments of a number of small organic molecules using a microwave spectrometer equipped with a magnet capable of producing fields up to 30 kG. With this type of spectrometer it is, however, not possible to determine the nuclear shielding effects. As these effects are proportional to the magnetic field they are below the resolving power of conventional microwave spectrometers.

A considerable reduction of the Doppler broadening is obtained when a molecular beam is used instead of the sample gas volume in conventional microwave spectrometers. The ultimate resolution of such a molecular beam absorption spectrometer is determined only by the uncertainly principle, if all broadening due to the Doppler effect and other instrumental effects is eliminated. However, all spectrometers in the microwave region using this technique have suffered from low sensitivity and have found little application. Gordon *et al* (Gor 55) showed that this limitation can be removed, in some cases, by

[1] In the following the energy of a molecule will be often expressed in kHz.

[2] The resolution of a spectrometer is expressed by the 'half-width' of the spectral lines. In the following 'half-width' stands for: 'half of the width of the line at half of its maximum intensity'.

the application of the maser principle. Another remedy is to operate the molecular beam absorption spectrometer at a higher frequency, since the sensitivity of such a spectrometer is proportional to the frequency (Hui 66). Both techniques, beam maser spectroscopy and beam absorption spectroscopy, are used with great success. The beam maser spectrometer has been used by Bluyssen (Blu 68) and by Verhoeven (Ver 69) to evaluate electric as well as magnetic properties of isotopic species of the water molecule. The millimeter wave beam spectrometer was used by Huiszoon and by van Dijk *et al* to determine the nuclear hyperfine properties of H_2S (Hui 66) and the nuclear hyperfine properties and the molecular electric dipole moments of the hydrogen bromide and hydrogen iodide molecules (Dijk 70, Dijk 70a). Both techniques can not be used for the hydrogen fluoride molecule however, since the lowest rotational transition lies at 1200 GHz, whereas the highest frequency in the millimeter range which can be produced at the present moment is 800 GHz (Hel 70).

With the molecular beam resonance method the transitions between the substates of a rotational state can be observed. The spectra obtained with this method are often called radio-frequency spectra as the transition frequencies lie in the MHz range. A difference between this method and the spectroscopic techniques mentioned above is that the spectral lines are observed as a change in the intensity of the molecular beam and not as a change in the intensity of the electromagnetic radiation. Two types of molecular beam resonance methods are known; the MBMR method and MBER method. In both methods quantum state selection of the molecular beam plays an important role. As will be shown in Sect. 1.3 the MBMR method can be applied to molecules which possess a magnetic dipole moment, whereas the MBER method can be applied to molecules which possess an electric dipole moment. As nearly all molecules, polar as well as nonpolar, possess a magnetic dipole moment, the MBMR method can be used for nearly all molecules. However, as will be shown in Sect. 1.4, the MBER method is preferable for polar molecules.

1.3 PRINCIPLE OF THE MOLECULAR BEAM RESONANCE METHOD

A molecular beam resonance apparatus generally consists of two or more evacuated compartments connected by small diaphragms. One compartment, the source chamber, contains a source of the molecular beam. The molecules in the source effuse through a narrow slit or circular hole of about 0.1 mm^2 area into the source chamber. Only a small fraction of the molecules (< 1 %) effuses in the direction of the molecular beam detector, and most of the gas effusing from the source is pumped away by the pumping system of the source chamber.

In the other compartment, the beam passes in succession an inhomogeneous

field (A-field), a homogeneous field region (C-field), and again an inhomogeneous field (B-field) The A- and B-fields are magnetic for MBMR, and electric for MBER In the first case the A- and B-fields deflect magnetic dipole moments, and in the second case electric dipole moments

The inhomogeneous A- and B-fields exert forces on the molecules of the beam The force $\mathbf{F}$ acting on a diatomic $^1\Sigma$– molecule is given by:

$$\mathbf{F} = -\,\mathbf{grad}\, W = -\,(\partial W/\partial E)\;\; \mathbf{grad}\, E = -\,\mu_{\mathrm{eff}}\;\; \mathbf{grad}\, E, \qquad (1\,1)$$

where W is the potential energy of the molecule in electric, or magnetic field, $\mathbf{E}$ with strength $|\mathbf{E}| = E$, and μ_{eff} is the effective dipole moment:

$$\mu_{\mathrm{eff}} = -\,g_J\,\mu_N\,m_J, \qquad (1\,2)$$

for magnetic dipoles, and

$$\mu_{\mathrm{eff}} = -\,\frac{3\,\mu_{\mathrm{el}}^2\,E}{hAJ\;(J-1)}\;\frac{3\,m_J^2 - J\,(J+1)}{3\,(2J-1)\,(2J+3)}, \qquad (1\,3)$$

for electric dipoles [3]

In Eqs (1 2) and (1 3) g_J is the molecular g-factor, μ_N is the nuclear magneton, μ_{el} is the electric dipole moment, A is the rotational constant, E is the external electric field, h is Plancks constant, J is the rotational quantum number, and m_J is the projection of $\mathbf{J}$ along the external field axis

The gradients of the fields in the A- and B-regions are adjusted in such a way that only molecules with a certain effective dipole moment $(\mu_{\mathrm{eff}})_1$ will reach the detector [4]

In the C-field region homogeneous electric and magnetic fields are applied, which interact with the molecules in the beam Radio-frequency (rf) radiation is also applied in the C-field region, a magnetic oscillatory field is used for MBMR and an electric oscillatory field for MBER. The field vector of the rf radiation is perpendicular to the molecular beam to eliminate line broadening due to the Doppler effect If the energy of the rf radiation is equal to the energy difference between the selected quantum state i and any other quantum state f with $(\mu_{\mathrm{eff}})_i \neq (\mu_{\mathrm{eff}})_i$, and if the dipole transition from state i to state f is allowed, the quantum state f will also be populated (Sect 3 5)

[3] For molecules which possess a strong Stark effect higher order terms must also be taken into account in Eq (1 3) This is the case for alkalihalide molecules (Lee 67)

[4] The molecules in the beam travel with different velocities and so the deflections in A- and B-fields will be different for different molecules However this will not influence the arguments

The molecules in quantum state f will be deflected, however, in the B-field along another path than the molecules in the quantum state i as $(\mu_{eff})_f \neq (\mu_{eff})_i$. The direct result will be a change in the intensity of the molecular beam at the detector. So, besides the selection rules of dipole moment transitions, the spectra are also governed by the observational criterion (machine rule), which requires a change in μ_{eff} As the rotational quantum number J is unchanged in radio-frequency spectra the machine rule is fulfilled if $\Delta m_J = \pm 1$.

1 4 FEATURES OF THE MBER AND MBMR METHODS

The high resolution and the high sensitivity at radio-frequencies are the important features of MBER and MBMR spectrometers. The resolution is determined by the length of the resonance region according the relation $\Delta\nu = 1/\Delta\tau$ where $\Delta\nu$ is the half-width of the spectral line and $\Delta\tau$ is the transit time of the molecules through the resonance region. If instrumental effects such as inhomogeneity in the electric and magnetic fields in the C-field region are sufficiently small, a half- width of a few kHz is readily obtainable

The sensitivity of the spectrometer depends on the detection efficiency of the molecular beam detector and on the acceptance angle of the A- and B-fields (Sect. 2.2.2) Most MBER spectrometers employ electric 4-pole fields as state selecting devices (Dre 61, Wac 67) It can be easily shown that the radial force acting on a diatomic molecule in an electric quadrupole field, is harmonic (Ben 55, Wac 67). This means that the selected molecules in the beam are focussed on the detector and not only deflected. The acceptance angle of a quadrupole field is much larger than the acceptance angle of a dipole field (Rabi-type) So the use of quadrupoles increases the sensitivity of a MBER spectrometer

As shown in Eq (1.2), the effective dipole moment in MBMR spectroscopy is determined only by the quantum number m_J; so for low m_J-values many rotational states, when populated thermally according to the Maxwell-Boltzmann formula, will reach the detector. In this case, a broadening and a shift of the spectral lines occurs, as the electric and magnetic properties of molecules are slightly J-dependent (Sect. 5 2) This broadening does not occur in MBER experiments, as the molecules are selected for m_J as well as for J (Eq. 1.3) Therefore, for polar molecules, MBER spectroscopy is preferable over MBMR spectroscopy.

THE APPARATUS

2.1 GENERAL FEATURES

The present MBER spectrometer is a newly built version of the machine used by Van Wachem (Wac 67). New features are the introduction of a long resonance region, a magnetic field in this region, a universal molecular beam detector, and quadrupole fields which can sustain high electric field strengths.

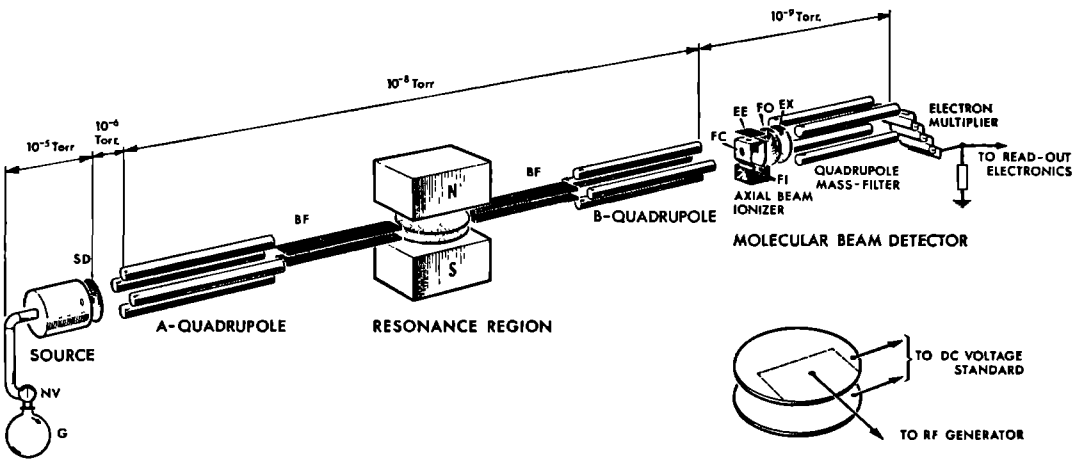

FIG. 2.1 Schematic diagram of the spectrometer. (*G*) gas reservoir, (*NV*) needle valve, (*SD*) source diaphragm, (*BF*) buffer field, (*FI*) filament, (*FC*) Faraday cage, (*EE*) electron extractor, (*FO*) focus lens, (*EX*) exit lens.

A schematic diagram of the spectrometer is given in Fig. 2.1. The main components of the spectrometer are: the source, the *A*-field (*A*-quadrupole), the *C*-field condenser, the electromagnet, the *B*-field (*B*-quadrupole) and the molecular beam detector. The components of the spectrometer, except the electromagnet, are housed in six stainless steel, argon arc welded, vacuum chambers. The chambers are, in order from source to detector: the source chamber, the buffer chamber, the *A*-quadrupole chamber, the *C*-field chamber, the *B*-quadrupole chamber, and the detector chamber. Special features of the various vacuum chambers will be given with the description of the components inside

that vacuum chamber. The *C*-field chamber is supported by a stainless steel frame, whereas the other vacuum chambers rest on two iron frames. The alignment of the components of the beam transmission system inside the vacuum chambers is performed optically using a telescope.

Various sources were used: a source for the production of alkali-halide beams for the maximum temperature of about 1100° K (Lee 68a), a low temperature source for the region 80°–300° K for the measurements on OCS and HCl, and a teflon source (Lee 70b) for the measurements on HF. All sources were adjustable from outside the vacuum system and were operated at conventional flow rates on the order of 10^{-2}Torr·l·s^{-1}. The source chamber and the *A*-quadrupole chamber are isolated from each other by a buffer chamber. To isolate chambers with different pressures, diaphragms are placed between them.

Electric quadrupole fields (Sect. 2.2) are used for the state selection of the molecular beam. Each quadrupole field consists of four cylindrical rods, the configuration of the four rods closely approximating the hyperbolic surfaces of a true quadrupole field. The focussing properties for polar diatomic $^1\Sigma$–molecules with Maxwell-Boltzmann velocity distribution are discussed in Sect. 2.2.2. The quadrupole fields are very precisely constructed and sustain a field strength of 270 kV/cm between two neighbouring rods before breakdown takes place. With these quadrupoles it was possible to focus a molecular beam of carbon monoxide molecules. The electric dipole moment of this molecule is only 0.1 D (Bur 58).

A condenser (Sect. 2.3) is used for the application of the static homogeneous electric field and the radio-frequency (*rf*) radiation to the molecules of the beam. The static electric field is made very homogeneous by using optically flat quartz disks, coated with gold, as the plates of the condenser. The method of the application of the *rf* radiation was critically examined (Sect. 2.3.1). A slit shaped region in the coating of one of the plates (Fig. 2.1) allows the application of the *rf* radiation to a 20 cm path along the beam axis. The slit is coated slightly to prevent any influence of the slit on the homogeneity of the static field.

A *C*-type electromagnet (Sect. 2.7) is used for the application of the static homogeneous magnetic field at the resonance region. The magnet is mounted outside the vacuum system on a carriage which travels on rails. The stainless steel *C*-field chamber fits in the gap of the magnet. The very homogeneous magnetic field allows the observation of Zeeman effects up to 4 MHz at half-widths of 600 Hz.

A commercial EAI Quad 250 Residual Gas Analyzer (RGA), with its associated equipment, is used as the molecular beam detector (Sect. 2.6). The RGA consists of an electron bombardment ionizer, a quadrupole mass filter, and an

electron multiplier. The RGA is housed in an ultrahigh vacuum system to reduce background currents due to ionized residual gasses.

A constant electric field, also called buffer field, (Sect. 2.5, Fig. 2.1) is applied to the molecules between both quadrupoles and the *C*-field condenser to preserve their spatial orientation.

An adjustable beamstop (Sect. 2.4), which optically screens the detector opening from the source, is placed at the entrance of the *C*-field. The beamstop stops the molecules which travel along the symmetry axis of the quadrupoles. These molecules are not state selected, as the gradient of the electric field on the axis of the quadrupole is zero.

TABLE 2.1 Dimensions of the apparatus (in mm).

Distance from source to *A*-quadrupole	225
Length of quadrupoles	300
Distance between quadrupoles	1290
Length of buffer fields	482
Diameter of *C*-field plates	304
Distance from *B*-quadrupole to detector	350

Design considerations, construction and tests of the performance of the apparatus are the subjects of the following sections.

A list of the various components with the dimensions and their respective distances, can be found in Table 2.1. The pumps used, their effective pumping speeds, and the pressures in the vacuum chambers are given in Table 2.2.

TABLE 2.2 Effective pumping speeds and pressures.

	Effective pumping speed (l/s)	Pressure (Torr)
Source chamber	965[a]	1 — 5 × 10^{-5}[e]
Buffer chamber	70[b]	0.5 — 1.0 × 10^{-6}[f]
A-, *B*- and *C*-field chamber[h]	700[c]	3 × 10^{-8}[g,i]
Detector chamber[h]	250[d]	4 × 10^{-9}[g,i]

[a] Water baffled oil diffusion pump (*Leybold:* DO2001).
[b] Water baffled oil diffusion pump (*Leybold:* DO251), with extra uncooled baffle above the water cooled baffle, which optically screens the vacuum chamber from the pump system.
[c] Three ion getter pumps (*Leybold:* IZ250, IZ250, IZ200).
[d] Ion getter pump (*Leybold.* IZ250).
[e] Base pressure (no beam): $< 2 \times 10^{-6}$ Torr.
[f] Base pressure (no beam): $< 0.4 \times 10^{-6}$ Torr with liq. N_2 trap in the vacuum chamber.
[g] After baking for 24 h at approximately 150°C (*C*-field chamber: 60°C).
[h] The chamber(s) is (are) pumped with sorption pumps (*Riber.* 3 × PA 10) to the starting pressure of the ion getter pump(s).
[i] Estimated from the current to the pump.

2.2.1 *Design considerations and construction*

The *A*- and *B*-quadrupoles are made of highly polished stainless steel rods 7 mm in diameter. The inner diameter (*i.d.*) of the field region is 6 mm. For a given *i.d.* of the field region, the minimum length of the rods is dictated by the maximum voltage attainable across the rods, the velocity of the molecules in the beam, and the magnitude of the Stark effect (Lee 67). We have found that in a clean vacuum and with highly polished rods, a voltage of 60 kV can be maintained over a gap of 2.2 mm (Fey 68). With these quadrupoles we intended to focus CO molecules in their $J = 1$ state effusing from a source at 80° K, and higher rotational states of HF and HCl effusing from a source at 300° K. To accomplish this the quadrupoles were made 30 cm long (Lee 67, Lee 69d).

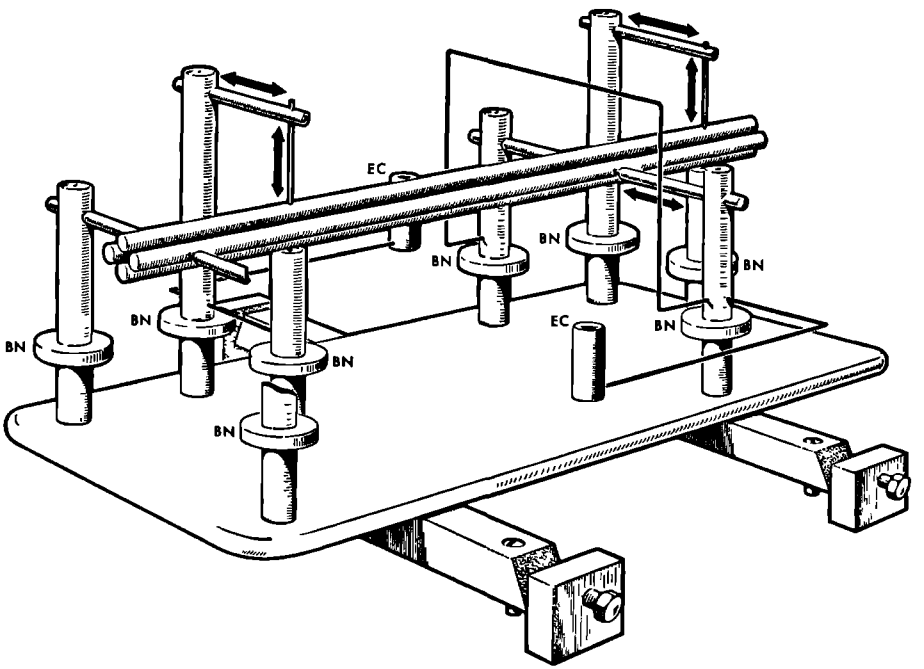

FIG. 2.2 Quadrupole. (*BN*) boron nitride insulator, (*EC*) electrical connection.

The construction of the quadrupoles is seen in Fig. 2.2. The insulators between the quadrupole rods and ground are made of boron nitride. Care must be taken to avoid exerting excessive torque on these insulators since they break easily. Small stainless steel rods are tightly fitted into the quadrupole

rods. These rods are mounted to a base plate by one or two auxilliary adjustable rods. In this way the quadrupole rods are held in position to within 0.2 mm. The final alignment of the quadrupole along the beam axis is achieved by adjusting the base plate.

Each quadrupole is housed in a vacuum chamber with *i.d.* of 340 mm and inner height of 210 mm. A large upper flange provides easy accessibility to the quadrupole. The high voltages to the quadrupole rods are applied through ceramic seals (Frialit) mounted on the large upper flange. A viewing port and a metal valve are mounted on the side flanges of the quadrupole chambers. The viewing port permits observation of the quadrupole under operation in case of occasional arcing. The quadrupole chambers and the *C*-field chamber are sorption pumped to the starting pressure of the ion getter pumps. The large upper flange is gasketted with an aluminium wire (diameter 2.0 mm); all other flanges are sealed with Viton O-rings.

2.2.2 *Calculation of focussing properties*

Space focussing of polar diatomic molecules with electric quadrupole fields was introduced by Bennewitz, Paul and Schlier (Ben 55). Most properties were derived for monoenergetic beams (Ben 55, Wac 67). We have written a digital computer program, which calculates the intensities of space focussed beams with Maxwell-Boltzmann velocity distribution (Eve 69, Lee 69d). The results of these calculations are given below.

The solid angle $<\Omega>$ at the source opening, within which the molecules emerging from the source are focussed at the detector is given by:

$$<\Omega> = \frac{\int_0^\infty \Omega(v) I(v) dv}{\int_0^\infty I(v) dv}, \tag{2.1}$$

where $\Omega(v)$ is the solid angle at velocity v and $I(v)$ is the velocity distribution function (Ram 56, p. 20). The solid angle $\Omega(v)$ is defined as (Ben 55, Wac 67):

$$\Omega(v) = \pi (\gamma_{max}^2 - \gamma_{min}^2), \tag{2.2}$$

where γ_{max} and γ_{min} are the maximum and the minimum angles (defined with respect to the molecular beam axis) between which the molecules have to start at the source in order to reach the detector.

We have choosen the distance between the quadrupoles, the distance between

the B-quadrupole and the detector, and the diameter of the detector opening as free parameters in the calculation of $<\Omega>$. The calculation indicates that $<\Omega>$ varies by 10 % as these two distances were varied between 30 and 160 cm and 20 and 40 cm, respectively. The present values are 129 cm and 35 cm. The solid angle $<\Omega>$ had its maximum value of 53×10^{-6}sr at a detector opening of 2.0 mm.

The molecules, which undergo a transition into a non-focussable state in the resonance region, but nevertheless are not completely defocussed in the B-quadrupole, give a decrease of the spectral line intensity. To describe this effect the quantity $<\Omega_1>$ is introduced defined as:

$$<\Omega_1> = \frac{\int_0^\infty \{\Omega(\nu) - \Omega'(\nu)\} I(\nu)\, P_{p,q}(\nu)\, d\nu}{\int_0^\infty I(\nu)\, d\nu} . \tag{2.3}$$

In this expression $\Omega'(\nu)$ is the solid angle for molecules which enter the B-quadrupole region in a non-focussing state and yet strike the detector, and $P_{p,q}(\nu)$ is the transition probability function (Ram 56, p. 119; Sect. 3.5). In the present experiments $<\Omega_1> \approx 0.8 <\Omega>$.

2.2.3 *Performance*

The voltages to the quadrupole rods are taken from regulated power supplies with a maximum voltage of 30 kV (Brandenburg). Opposite rods of the quadrupole are held at the same voltage, one set of opposing rods is at a positive voltage, the other one at a negative voltage (Fig. 2.2). The current to the rods was monitored. If the rods are clean and well polished the current to the rods is below 100 μA when ± 30 kV is applied to the rods. When the current exceeded this value, the quadrupole was removed from the apparatus and the rods were repolished and cleaned.

From the solid angle $<\Omega>$ (Sect. 2.2.2) we have calculated the line intensity of the $^{16}O^{12}C^{32}S$ resonance line $J = 1 \rightarrow 1$, $m_J = 0 \rightarrow \pm 1$ at a source temperature of 150°K and a full beam signal I_b (full beam = beam stop off-axis and no voltages on the quadrupole rods). The fosussed beam intensity I_f is given by

$$I_f = \frac{<\Omega>}{\Omega_{det}} \eta I_b, \tag{2.4}$$

where Ω_{det} is the solid angle of the detector from the source ($\Omega_{det} = 0.51 \times 10^{-6}$sr), and η is the population of the quantum state involved ($\eta = 0.0019$).

This gives $I_f = 0.2\ I_b$. Because of the contribution of $<\Omega'>$ (Sect. 2.2.2) the line intensity will be about 20 % lower. The observed results for $<\Omega>$ and $<\Omega_1>$ were about 40 % lower than the calculated values. Keeping in mind the complexity of the calculations, one may state that the agreement is rather good.

With the present quadrupoles the $J = 1$, $m_J = 0$ state of carbon monoxide was focussed and the electric dipole moment was determined from the observed Stark spectrum. The result was $\mu_{el} = 0.1086\ (1)$ D (Lee 70c).

2.3 THE C-FIELD

2.3.1 *Design considerations and construction*

The *C*-field condenser consists basically of two optically flat quartz plates (Van Keuren), 304 mm in diameter and 25 mm thick (Fig. 2.3). One of the surfaces of each plate is ground to an accuracy of 800 Å concave. The ground surfaces are separated by three quartz spacers, 25 mm in diameter. The accuracy of the bottom surface and the top surface of each spacer is 300 Å convex. The surfaces of each of the spacers are parallel to within 300 Å. Their thickness is 6.36362 ± 0.00002 mm.

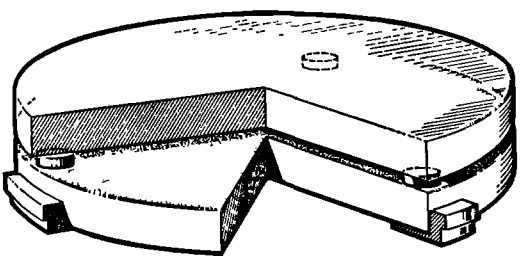

FIG. 2.3 *C*-field.

The ground surfaces of the quartz plates are coated in vacuum, except at those regions where the spacers would come in contact with the coated surfaces. The coating procedure is described below. A slit shaped region in the coating of one of the plates allows for the application of the *rf* field to a 20 cm path along the beam axis (Fig. 2.1). We have calculated, and also deduced from experiments, that an uncoated slit causes an inhomogeneity in the electric field of the order of 10^{-4} (Mee 69, Lee 69c). This inhomogeneity causes a shift and a broadening of the spectral lines. However, a slightly conducting slit reduces the inhomogeneity to within only 3 ppm (Sect. 2.3.2).

Prior to coating the quartz plates were repolished and bombarded with ions for ten minutes. The electrode on which the ions were collected was an alumi-

nium rod wrapped in clean aluminium foil. The current to the electrode was 50 mA, at a voltage of about —3 kV with respect to the base plate of the coating apparatus and a pressure of 2×10^{-2} Torr. At a pressure below about 5×10^{-6} Torr the plate was coated with a very thin aluminium film. A mask, which had the form of the slit, was then brought into position, and the plate was recoated with a gold film with an optical transmission of 10 %. The mask was then removed and the plate was coated again with a gold film until the slit resistance was about 200 Ω. Thin wires were soldered with indium to small coated areas at the periphery of the regions separated by the slit in order to monitor the resistance of the slit. The surface resistance of each of the sections was approximately 20 Ω. The resistance of the slit may increase within a week by a few orders of magnitude of the original value. Occasionally the application of voltage to the *C*-field causes a decrease in the slit resistance. These processes are not well understood.

To eliminate variation of the separation due to bending of the quartz plates (Dew 66), the following steps are performed (Fig. 2.3). The bottom plate is supported at three points in a stainless steel ring placed in the *C*-field chamber. The spacers are positioned above these points of support. On these spacers the upper plate is placed. So the bending pattern will be the same for both quartz plates. The stainless steel ring allows for the adjustment of the position and the orientation of the *C*-field condenser with respect to the beam axis.

The *C*-field vacuum chamber is 74 mm high. It has a large upper flange, 6 mm thick, which provides good access to the *C*-field. The direct (*dc*) and *rf* voltages to the *C*-field condenser are applied through ceramic seals. The chamber and the upper flange are made of stainless steel, with a relative permeability of unity to within 3×10^{-3}. All flanges are sealed with Viton O-rings.

2.3.2 *Performance*

We checked the parallelism of the coated surfaces with the aid of Haidinger fringes in reflected sodium light. The variation in the distance between the coated surfaces was less than one quarter of a wavelength. The variation along the beam path was reduced to less than one tenth of a wavelength by exerting constant external forces on the plates.

The homogeneity of the electric field and the shift of the lines on changing the polarity of the field was tested by observing the OCS resonance $J = 1 \rightarrow 1$, $m_J = 0 \rightarrow \pm 1$ at 800, 1199.4, and 1571.22 V/cm. In this experiment no aluminium film, prior to the coating with gold, was deposited on the plates. The experimental results are given in Table 2.3. It is seen from this table that the

TABLE 2.3 Carbonyl sulphide ($^{16}O^{12}C^{32}S$) resonances $J = 1 \rightarrow 1$, $m_J = 0 \rightarrow \pm 1$ at different electric field strengths. The measurements are performed in the ground vibrational state.

E (V/cm)	ν_+[a] (kHz)	ν_-[b] (kHz)	$(\nu_+ + \nu_-)/2$ (kHz)	$\Delta\nu$[c] (kHz)
800	2044.80 ± 0.07	2044.79 ± 0.07	2044.80 ± 0.05	0.65
1199.4	4595.21 ± 0.07	4595.29 ± 0.07	4595.25 ± 0.05	0.68
1571.22	7884.07 ± 0.07	7884.06 ± 0.07	7884.06 ± 0.05	0.70

[a] ν_+ — resonance frequencies with upper plate of C-field at positive potential with respect to the lower plate.
[b] ν_- — resonance frequencies with upper plate of C-field at negative potential with respect to the lower plate.
[c] $\Delta\nu$ — half-width.

observed resonance frequencies did not depend on the direction of the applied electric field. Only a small line broadening was observed at the highest field strength. This line broadening can be explained by the residual variation of about 600 Å in the distance between the plates along the beam axis. With these plates the maximum field strengths at which measurements could be done was 2000 V/cm. At higher field strengths the gold film around the slit peeled off and the slit resistance became infinite. This peel-off did not occur when the plates were ion-bombarded and aluminium-coated, prior to the coating with gold.

2.4 THE BEAMSTOP

The beamstop is mounted in the C-field vacuum chamber. It consists of a tin droplet, 1.2 mm in diameter, soldered on a 0.2 mm copper wire. The wire is mounted on a U-shaped stainless steel plate. Two cam and rider assemblies, controlled from the outside, adjust the horizontal and the vertical positions of the beamstop.

2.5 THE BUFFER FIELDS

A constant electric buffer-field (Fig. 2.1) is applied to the molecules between both quadrupoles and the C-field condenser in order to preserve their spatial orientation.

Each of the two buffer fields is produced by two flat horizontal stainless steel plates, 8 mm thick, 482 mm long, and 30 mm wide. The distance between the plates is 6.36 ±0.01 mm. The plates are fastened to aluminium oxide strips, which are in turn separated, outside the electric buffer field, by aluminium oxide tubes. Each of the buffer field assemblies is supported in the quadrupole

chamber and in the *C*-field chamber. The adjustment of the fields along the molecular beam axis is achieved by moving the supports. The voltages to the buffer fields are applied through ceramic seals mounted on the *C*-field chamber. The buffer fields described above permit extension of the *C*-field up to 120 cm. No experiments with such a long *C*-field have been performed so far.

2.6 THE MOLECULAR BEAM DETECTOR

The molecular beam detector is a commercial EAI Quad 250 Residual Gas Analyzer (RGA) with its associated electronic equipment. The analyzer head consists of an electron bombardment (EB) ionizer, an ion lens system, a quadrupole mass filter and a 14 stage Cu-Be multiplier.

The performance of the RGA, as a molecular beam detector was investigated using a KCl beam (Lee 68b). The most probable velocity of the beam molecules was 580 m/s. The intensity of the beam was measured with a tungsten surface ionization (SI)-detector. This SI-detector was placed before the EB-detector. Both detectors were operated using the same detector opening, 0.3 mm in diameter. At a beam intensity of 7.5×10^7 mol/s, as calculated from the signal of the SI-detector, we obtained a current of 6×10^{-13}A at the output of the multiplier. At a nominal gain of the multiplier of 10^4, this means that, for every 2×10^5 molecules which enter the ionizer only one ion reaches the first dynode of the multiplier.

In this investigation the typical beam intensity at the detector was 10^{11} mol/s. This results in an output current of the multiplier of 10^{-9}A. At this current the noise was 4×10^{-12}A peak to peak at a time constant of 1s of the read-out system. The current due to ionized residual gas could in most cases be neglected.

The measured line intensity for the $^{16}O^{12}C^{32}S$ resonance line $J = 1 \rightarrow 1$, $m_J = 0 \rightarrow \pm 1$ was about 0.1 I_b, where I_b is the full beam signal (Sect. 2.2.3). At $I_b = 10^{-9}$A, the signal to noise ratio of the resonance line is 25. A recording of the spectral line is given in Fig. 4.1.

2.7 THE ELECTROMAGNET

A *C*-type electromagnet (Bruker Physik) is used for the application of the static homogeneous magnetic field at the resonance region. The magnet is mounted on a carriage which can move on rails.

The tapered pole faces of the magnet are 24×50 cm. Iron shims are screwed to these faces to insure reduction of edge effects. The gap is 9 cm wide. Two 600 turn coils[1], made out of solid 2×11 mm wire, provide the magnetization

[1] (Smit Electrotechnical Factories)

of the yoke. The coils are connected in series, and their total cold resistance is 2.60 Ω. The coils were impregnated at the factory with epoxy in vacuum. Each coil is mounted between two water cooled brass plates. The coils are electrically insulated from the plates by a glass mica foil. Heat sink compound (Dow Corning No. 340) is used for optimum heat transfer from the coils to the brass plates.

At a current of 50 A the magnetic field in the gap was 8.7 kG. With a water flow rate through the brass plates of 700 l/h the average temperature in the coil is about 48°C. This increase was calculated from the increase in coil resistance and from the temperature coefficient of the wire which is 0.004/°C. The maximum and minimum local coil temperatures as measured at the outside of the coils were 75°C and 20°C, respectively. From these three temperatures, it can be concluded that there is no strong temperature gradient toward the inside of the coil. The maximum operating temperature of the coil is 120°C.

Graphs obtained at the Laboratory of Bruker Physik Company show that the variation in the field of the present magnet along the resonance region is less than 0.1 G at a field strength of 5 kG. The Zeeman effect measurement at 8.4 kG on HCl have shown a line broadening of 0.2 kHz, which corresponds to a residual variation of about 0.4 G.

The magnetic field is measured before and after each run with a NMR probe (Varian F-8 Fluxmeter). If the center frequency f_0 of the nuclear resonance signal is known, the value of the magnetic field B follows from the relation:

$$B = f_0/\gamma$$

where γ is the specific gyromagnetic ratio of the sample. A deuteron sample is used ($\gamma = 0.65360$ MHz/kG). The resolution of the fluxmeter allows a field determination to within 20 ppm at 8 kG. It was not possible to measure the field at the position of the molecular beam. From experiments it was felt that the field was known to within 2×10^{-4}. This feeling was rather well confirmed in the measurements on the HCl molecule (Sect. 5.6.2).

During the experiments in an external magnetic field one resonance was regularly observed to monitor the magnetic field during the runs. The typical fluctuation, mainly due to a change in the room temperature, was of the order of 0.12 G/h.

2.8 THE ELECTRONIC EQUIPMENT

The *dc* voltage to the *C*-field condenser was taken from a Fluke 332 A voltage standard. For high precision measurements the standard was calibrated by the Instrumentation Department of the Faculty to an accuracy of 3 ppm.

The *rf* voltage for the *C*-field was taken from a frequency synthesizer (Schomandl ND 30M, Hewlett Packard 5105A) and was amplified, if necessary. An electronic counter was connected to the synthesizer for the production of frequency markers. In cases when the resonance lines were observed as a variation of the direct beam intensity, the output current from the electron multiplier was amplified with a Cary vibrating reed electrometer (Model 31) or a Keithly electrometer (Model 610). The *dc* output signal of these electrometers was fed to a Servogor recorder (Model RS 411) along with the frequency markers.

In some cases the *rf* voltage for the *C*-field was 100 % modulated at 30 Hz. The *ac* output voltage of the electron multiplier, which is proportional to the intensity of the resonance, was amplified in a Keithly 610 electrometer and measured with a PAR JB5 phase sensitive detector. The *dc* output signal of the phase sensitive detector was fed to the recorder along with the frequency markers.

The spectra were measured with a sweep rate of about 10 to 50 Hz per second. Each experimental line was measured twice, once sweeping from high frequency to low and once from low to high frequency, in order to minimize the effect of time constant on line position.

THEORY OF THE SPECTRA

3.1 INTRODUCTION

The Hamiltonian which describes the interaction of nuclear moments in a rotating $^1\Sigma$-diatomic molecule with the internal fields and the interaction of nuclear moments and molecular charge and current distributions with an external magnetic field, has been investigated extensively in the past decades. The molecular beam experiments on isotopic species of the hydrogen molecule (Kel 39, Ram 40, Bar 54, Qui 58) have led to a Hamiltonian which describes these interactions very well. The terms of this Hamiltonian were written essentially in terms of certain coupling constants, of the external magnetic field **B**, and of quantum mechanical operators which were functions of the rotational angular momentum vector **J** and of the nuclear spin vector **I**. The terms relevant to the interaction of the molecular charge distribution with an external electric field **E**, were subsequently added to the Hamiltonian of Ramsey. Schlier (Sch 61) has shown that the Hamiltonian extended in this way contains all interactions which can be constructed from the vectors **I**, **J**, **E**, and **B**, as far as they can be measured with a molecular beam resonance apparatus.

The half-widths of the spectral lines measured in this work are on the order of 600–1200 Hz. This is 2–4 times the half-widths of the spectral lines in the experiments on the hydrogen molecule. It is therefore expected that the spectra from this work can be interpreted very well with the Hamiltonian given by Ramsey and his collaborators (Bar 54, Qui 58). The interaction of the magnetic octupole moment of the chlorine nucleus in the HCl molecule with the second derivative of the internal magnetic field will contribute less than 10 Hz to the energy of the molecule (Lee 70c). This contribution can not be resolved with the present spectrometer and is therefore neglected.

In this work tensor notation of the Hamiltonian (Gün 54, Tha 64, Dym 66, Hüt 67, Heu 68, Ver 69) is used instead of the original form (Bar 54, Qui 58). The techniques of spherical tensor operators (Edm 60, Jud 63) can then be used for the calculation of the matrix elements (Hui 66, Wac 67, Blu 68, Ver 69).

3.2.1 *The Hamiltonian*

The Hamiltonian of a diatomic polar molecule in the electronic $^1\Sigma$-state with nonzero nuclear spins in an external electric field **E** and a magnetic field **B** has the following form:

$$\mathbf{H} = \mathbf{H}_0 + AJ^2 - \mu_{el} \cdot \mathbf{E} - \tfrac{1}{2}\mathbf{E} \cdot \alpha \cdot \mathbf{E} - \mathbf{B} \cdot \mathbf{G} \cdot \mathbf{J} - \tfrac{1}{2}\mathbf{B} \cdot \chi \cdot \mathbf{B}$$
$$- \sum_K \frac{\mu_K}{I_K} \mathbf{I}_K \cdot (1 - \sigma_K) \cdot \mathbf{B} + \sum_K \mathbf{I}_K \cdot \mathbf{M}_K \cdot \mathbf{J} + \sum_K \sum_{L>K} \mathbf{I}_K \cdot \mathbf{D}_{KL} \cdot \mathbf{I}_L$$
$$+ \sum_K \mathbf{Q}_K : \mathbf{V}_K \qquad (3.1)$$

The average value of the operator $\mathbf{H}_0$ in Eq. (3.1) gives the sum of the electronic and vibrational energy of the molecule. These energies are not of interest in the present study and will not be discussed further. The other terms describe in this order the contribution to the energy of the molecule because of molecular rotation, Stark effect, electric polarizability, molecular Zeeman effect, magnetic susceptibility, nuclear Zeeman effect, spin-rotation interaction, spin-spin interaction, and quadrupole interaction.

The quantities which appear in Eq. (3.1) are: the rotational constant A of the molecule (Tow 55, p. 10), the operator of the total angular momentum **J** (neglecting nuclear spins), the electric dipole moment μ_{el}, the polarizability tensor α, the rotational magnetic dipole tensor **G**, the magnetic susceptibility tensor χ, the nuclear magnetic dipole moment μ_K of nucleus K with spin I_K, the nuclear shielding tensor σ, the nuclear spin-rotation tensor **M**, the nuclear spin-spin tensor $\mathbf{D}_{KL}$, the nuclear quadrupole tensor $\mathbf{Q}_K$, and the molecular electric gradient tensor $\mathbf{V}_K$.

The relevant expressions for the diagonal components of the molecular tensors **G**, χ, σ_K and $\mathbf{M}_K$ of a $^1\Sigma$-diatomic molecule defined with respect to axes parallel and perpendicular to the molecular z-axis, are listed in Table 3.1 in terms of nuclear coordinates, electronic coordinates, and off diagonal matrix elements of the total electronic orbital angular momentum. The expressions of the tensors α, $\mathbf{D}_{KL}$, $\mathbf{Q}_K$, and $\mathbf{V}_K$, which contributions are outside the scope of the present investigation, can be found elsewhere (Kol 67, Ver 69, Ram 56, p. 57).

In Table 3.1 the subscribt i runs over electrons and the subscripts K and L run over nuclei. Radius vectors with respect to the molecular center of mass are denoted by **r**. The length of **r** is given by $|\mathbf{r}| = r$, and $\mathbf{r}_{iK} = \mathbf{r}_i - \mathbf{r}_K$. Charge

TABLE 3.1 The diagonal components of the molecular tensors G, χ, σ_K, and M_K of a $^1\Sigma$ diatomic molecule defined with respect to the molecule fixed system. The molecular axis is denoted by z.

$$\mathbf{G} = \mathbf{G}^n + \mathbf{G}^e; \chi = \chi^n + \chi^d + \chi^p$$

$$\mathbf{M}_K = \mathbf{M}_K^n + \mathbf{M}_K^e; \sigma_K = \sigma_K^d + \sigma_K^p$$

$$G_{xx}^n = \frac{2\pi eA}{h} \sum_K Z_K r_K^2,$$

$$G_{xx}^e = -4\mu_B A \sum_{n\neq o} \frac{|<o|L_x|n>|^2}{E_n - E_o},$$

$$\chi_{gg}^n = -\frac{e^2}{4} \sum_K \frac{Z_K^2}{m_K} \{r_K^2 - (\mathbf{r}_K)_g^2\},$$

$$\chi_{gg}^d = -\frac{e^2}{4m} <o|\Sigma_i\{r_i^2 - (\mathbf{r}_i)_g^2\}|o>,$$

$$\chi_{xx}^p = 2\mu_B^2 \sum_{n\neq o} \frac{|<o|L_x|n>|^2}{E_n - E_o},$$

$$(M_K)_{xx}^n = -\frac{e\mu_o\mu_N g_K A}{h} \sum_{L\neq K} \frac{Z_L}{r_{LK}},$$

$$(M_K)_{xx}^e = \frac{\mu_o\mu_B\mu_N g_K A}{\pi} \sum_{n\neq o} \frac{<o|Q_x|n><n|Q_x'|o> + \text{c.c.}}{E_n - E_o},$$

$$(\sigma_K)_{gg}^d = \frac{e^2\mu_o}{8\pi m} <o|\Sigma_i r_{iK}^{-3} \{r_{iK}^2 - (\mathbf{r}_{iK})_g^2|o>,$$

$$(\sigma_K)_{xx}^p = -\frac{\mu_o\mu_B^2}{2\pi} \sum_{n\neq o} \frac{<o|Q_x|n><n|Q_x'|o> + \text{c.c.}}{E_n - E_o}.$$

and mass of nucleus L are $Z_L e$ and m_L, respectively. The electronic mass is m. The electronic ground state is $|o>$, with corresponding energy E_o. The electronic excited states are denoted by $|n>$ and their energies by E_n. The x-component of the total electronic orbital angular momentum with respect to the center of mass of the molecule is L_x. The latter operator is denoted by Q_x when it is defined with respect to a nucleus. The quantity $\mathbf{Q}'$ is defined as: $\mathbf{Q}' = \Sigma_i \mathbf{Q}_i/(r_{ik})^3$. The remaining quantities are: the permeability in vacuum $\mu_o = 4 \times 10^{-7}$ H/m, the nuclear magneton $\mu_N = 5.050951 \times 10^{-27}$ A·m^2, the Bohr magneton $\mu_B = 9.274096 \times 10^{-24}$A·m^2, Plancks constant h = 6.626196 $\times 10^{-34}$J·s, the gyromagnetic ratio of nucleus K defined by $g_K = (\mu_K/\mu_N)I_K$. All quantities are in MKSA units.

3.2.2 *Discussion of the Hamiltonian*

The explicit expressions in Table 3.1 have been obtained by several authors (Gün 54, Tow 55, Ram 56, Dre 61, Dym 66, Hüt 67, Heu 68, Ver 69) using the Born-Oppenheimer approximation, the rigid-rotor harmonic-oscillator approximation, and the assumption that the molecular center of mass coincides with the nuclear center of mass. In all calculations terms which give energy contributions smaller than the rotational energy of the molecule are treated as perturbations. The Hamiltonian of Eq. (3.1) contains both the first order (diamagnetic) and the second order (paramagnetic) contributions with respect to the electronic states.

The second order magnetic contributions arise from the perturbation of the electronic ground state by the molecular rotation. The paramagnetic contribution to the magnetic susceptibility was already recognized by Van Vleck (Vle 32, Chap. 10), in his treatment of the para- and diamagnetism of free molecules. The electronic contribution to the rotational magnetic moment was introduced by Ramsey (Ram 40) and by Wick (Wic 48). One consequence of these theories is the close relationship between the electronic contribution to the rotational magnetic moment and the paramagnetic contribution to the magnetic susceptibility. The close relationship might appear at first sight to be a surprising accident. However, it can be made quite reasonable from Larmor's theorem as pointed out by Ramsey (Ram 56, p. 164).

The diamagnetic shielding was calculated first by Lamb (Lam 41). The effect is described as follows. When an external magnetic field B is applied to an atom or molecule, the electrons acquire an induced diamagnetic circulation $-\sigma_{Av}^{d}B$ at the position of the nucleus which partially cancels the initially applied field. The quantity σ_{Av}^{d} is called the average diamagnetic shielding constant. Since the induced diamagnetic field is proportional to the magnetic

field originally applied, it cannot be distinguished from it by varying the magnitude of the field. Consequently, the nuclear shielding must be calculated theoretically if the actual nuclear moment is evaluated. Lamb's theory originally applies only to atoms, but was also used for molecules as no better theory was available at that time. However, it was pointed out by Ramsey (Ram 50a) that the paramagnetic contribution to the nuclear magnetic shielding could not be neglected in high precision molecular beam resonance experiments. Essentially, the paramagnetic contribution to the nuclear shielding, in the same way as the paramagnetic susceptibility, originates from the perturbation of the electronic ground state by the molecular rotation. The effect of nuclear magnetic shielding is particularly important in nuclear magnetic resonance (nmr) spectroscopy. As the nuclear shielding depends on the electronic charge distribution around the atom, it will be different in different molecules. This effect is known as 'chemical shift'. In molecular beam resonance experiments the molecules are not subject to frequent collisions. Consequently the shielding can be observed in different molecular states (Sect. 3.3), which is not possible in nmr spectroscopy.

The theory of spin-rotational interaction has been developed by Wick (Wic 48), Ramsey (Ram 50a), and White (Whi 55). One consequence of these theories is the close relationship between the electronic contribution to the spin-rotation magnetic interaction and the paramagnetic contribution to the magnetic shielding. Also this relationship can be made reasonable (Ram 56, p. 164).

The nuclear quadrupole interaction is well known (Tow 55, Chapt. 6). The interaction was detected in molecules for the first time by Kellogg *et al* (Kel 39) in the molecular beam resonance experiment on D_2. The direct result of this experiment was the quadrupole moment of the deuteron nucleus.

The nuclear spin-spin interaction consists of the direct interaction between two nuclear magnetic dipoles and of the electron coupled (indirect) interaction (Ram 53). The latter interaction has only been detected in a few molecules (Bar 54, Dre 61, Mue 70).

The typical contributions to the energy of a molecule, because of the nuclear quadrupole, nuclear spin-rotation and nuclear spin-spin interaction are: 0.1–1000 MHz, 1–500 kHz, and 1–50 kHz, respectively.

3.3 MATRIX ELEMENTS, ENERGY LEVELS, AND COUPLING CONSTANTS OF $^{16}O^{12}C^{32}S$, $^{16}O^{12}C^{34}S$, AND $^{16}O^{13}C^{32}S$ [1]

The most appropriate coordinate system for the calculation of the matrix elements of Eq. (3.1) is the space fixed center of mass system. If the space fixed

[1] The theory in this chapter is devoted to diatomic $^1\Sigma$-molecules. However, the theory is also valid for triatomic linear molecules, like OCS, in their ground vibrational state.

z-axis is choosen along the positive direction of the homogeneous external electric and magnetic field, $M = m_J + m_I$ will be a 'good' quantum number. The quantities m_J and m_I are the projections of **J** and **I** (of nucleus ^{13}C) along the space fixed z-axis. The relative energies of the spinless species $^{16}O^{12}C^{32}S$ and $^{16}O^{12}C^{34}S$ are found by omitting the terms which give the contributions due to the nuclear interactions.

The first order Stark effect is zero in a $^1\Sigma$ diatomic molecule. However, the second order Stark effect can be quite strong especially in those cases where the rotational energy levels are close to each other.

The spin-rotation interaction of the ^{13}C-nucleus in OCS contributes only a few kHz to the energy of the molecule. Therefore the coupling between **J** and **I** will be broken even at not to high magnetic or electric fields.

The matrix elements of the Hamiltonian of the $O^{13}CS$ molecule are calculated in a representation which diagonalizes the rotational and Stark Hamiltonian $A\mathbf{J}^2 - \mu_{el}\cdot\mathbf{E}$. The representation is given by (Mes 62, Chap. 16, Lee 67a):

$$\widetilde{|Jm_J>|Im_I>} = N|Im_I>\{|Jm_J> + \sum_i \sum_{J'\neq J} a_{J'}^{(i)}|J'm_J>\}, \qquad (3.2)$$

where $a_{J'}^{(i)}$ are coëfficients proportional to powers of $\mu_{el}E/hA$, N is the normalization constant, and i denotes the order of the perturbation. The second order Stark effect of the $J = 1$ level is calculated by taking $J' = 0,2$ and $i = 1$ in Eq. (3.2). Explicit expressions for $a_{J'}^{(i)}$ and $\widetilde{N}$ up to $i = 7$ are given elsewhere (Lee 67a). Henceforth, the representation $|\,Jm_J> |\,Im_I>$ will be abbreviated as $|\,m_Jm_I>$.

The method of the calculation of the matrix elements is outlined below, with the operator $\mathbf{B}\cdot\chi\cdot\mathbf{B}$ taken as an example. The operator $\mathbf{B}\cdot\chi\cdot\mathbf{B}$ is expanded in spherical components as (Hui 66, p. 66):

$$\mathbf{B}\cdot\chi\cdot\mathbf{B} = \sum_{k=0,1,2} (-1)^k\,(2k+1)^{\frac{1}{2}}\,\{B^{(1)}\,\{\chi^{(k)}\,B^{(1)}\}^{(1)}\}^{(0)}, \qquad (3.3)$$

where the spherical components of $\chi^{(k)}$, in terms of the Cartesian components, are given by (Yut 62, p. 106):

$$\begin{aligned}
\chi_0^{(0)} &= -(3)^{-\frac{1}{2}}(\chi_{xx}+\chi_{yy}+\chi_{zz}),\\
\chi_{\pm 1}^{(1)} &= \mp(2)^{-\frac{1}{2}}\{(\chi_{yz}-\chi_{zy}) \mp i(\chi_{zx}-\chi_{xz})\},\\
\chi_0^{(1)} &= i(2)^{-\frac{1}{2}}(\chi_{xy}-\chi_{yx}),\\
\chi_{\pm 2}^{(2)} &= \tfrac{1}{2}\{(\chi_{xx}-\chi_{yy}) \pm i(\chi_{xy}+\chi_{yx})\},\\
\chi_{\pm 1}^{(2)} &= \tfrac{1}{2}\{\mp(\chi_{xz}+\chi_{zx}) - i(\chi_{yz}+\chi_{zy})\},\\
\chi_0^{(2)} &= (6)^{-\frac{1}{2}}(2\chi_{zz}-\chi_{xx}-\chi_{yy}),
\end{aligned} \qquad (3.4)$$

and the spherical components of the vector **B** as:

$$B^{(1)}_{\pm 1} = \mp (2)^{-\frac{1}{2}} (B_x \pm iB_y),$$
$$B^{(1)}_0 = B_z. \tag{3.5}$$

Using tensor operator techniques (Edm 60, Jud 63, Chap. 3) the matrix elements of $\mathbf{B} \cdot \chi \cdot \mathbf{B}$ for the same J state can be evaluated as follows:

$$\begin{aligned}
&<m_J m_I \mid \mathbf{B} \cdot \chi \cdot \mathbf{B} \mid m_J' m_I'> \\
&= \sum_{k=0,1,2} \delta(m_I', m_I)\, B^2\, (2k+1)^{\frac{1}{2}} \begin{pmatrix} k & 1 & 1 \\ 0 & 0 & 0 \end{pmatrix} < m_J \mid \tilde{\chi}^{(k)}_0 \mid m_J'> \\
&= \sum_{k=0,1,2} (-1)^{J-m_J}\, \delta(m_I', m_I)\, \delta(m_J', m_J)\, B^2\, (2k+1)^{\frac{1}{2}} \begin{pmatrix} k & 1 & 1 \\ 0 & 0 & 0 \end{pmatrix} \begin{pmatrix} J & k & J \\ -m_J & 0 & m_J \end{pmatrix} \times \\
&<J \,||\, \chi^{(k)} \,||\, J>,
\end{aligned} \tag{3.6}$$

where $\tilde{\chi}^{(k)}_q$ are the components of χ in the space-fixed frame.

The reduced matrix element in Eq. (3.6) is evaluated with the aid of the Wigner-Eckart theorem. The relations between the components $\tilde{\chi}^{(k)}_q$ and the components $\chi^{(k)}_q$ of χ in the molecule fixed system are given by Messiah (Mes 62, p. 1075). The expression for the reduced matrix element in Eq. (3.6) and the components $\chi^{(k)}_q$ is given by (Lee 67a):

$$<J \,||\, \chi^{(k)} \,||\, J> = (-1)^J\, (2J+1) \begin{pmatrix} J & k & J \\ 0 & 0 & 0 \end{pmatrix} \chi^{(k)}_0. \tag{3.7}$$

Using the properties of the $3j$-symbols it follows from Eq. (3.7) that only terms with $k = 0,2$ contribute to the matrix element in Eq. (3.6). By using Eq. (3.4) and (3.7), the expressions for the matrix elements are:

$$\begin{aligned}
&<m_J m_I \mid \mathbf{B} \cdot \chi \cdot \mathbf{B} \mid m_J' m_I'> \\
&= \delta\,(m_I', m_I)\, \delta\,(m_J', m_J)\, B^2 \{\chi_{Av} - \frac{2\{3\, m_J^2 - J\,(J+1)\}}{3\,(2J+3)\,(2J-1)}\, (\chi_{//} - \chi_\perp)\},
\end{aligned} \tag{3.8}$$

where $\chi_{Av} = (3)^{\frac{1}{2}}\, (\chi_{xx} + \chi_{yy} + \chi_{zz})$,

and $\chi_{//} - \chi_\perp = \chi_{zz} - \chi_{xx}$.

The states with $J' \neq J$ in Eq. (3.2) also contribute to the matrix element of Eq. (3.8). An explicit calculation (Lee 69a) has shown that this contribution can be neglected.

The matrix elements of the other terms of the Hamiltonian are calculated by an analogous treatment. Explicit calculations are reported elsewhere (Lee 67a, Lee 70b). The energy W of a given $|Jm_J> |Im_I>$ state of the $O^{13}CS$ molecule up to fourth order in E and second order in B is:

$$W = \left[-\frac{3\mu_{el}^2 E^2}{2hAJ(J+1)} + (\alpha_{//} - \alpha_{\perp}) E^2 + (\chi_{//} - \chi_{\perp}) B^2 - 2(\sigma_{//} - \sigma_{\perp}) B m_I \frac{\mu_I}{I} \right] \times$$
$$\times \begin{pmatrix} 3m_J^2 - J(J+1) \\ 3(2J+3)(2J-1) \end{pmatrix} + \frac{\mu_{el}^4 E^4}{h^3 A^3} \left[-\frac{\{(J+1)^2 - m_J^2\}\{(J+2)^2 - m_J^2\}}{(2J+5)(2J+3)^3(J+1)^2(2J+1)} + \right.$$
$$+ \frac{\{(J+1)^2 - m_J^2\}^2}{(2J+3)^2(J+1)^3(2J+1)^2} + \frac{\{(J-1)^2 - m_J^2\}\{J^2 - m_J^2\}}{(2J-3)(2J+1)J^2(2J-1)^3} -$$
$$\left. - \frac{\{J^2 - m_J^2\}^2}{(2J+1)^2 J^3 (2J-1)^2} + \frac{\{(J+1)^2 - m_J^2\}\{J^2 - m_J^2\}}{(2J+3)(J+1)^2(2J+1)^2 J^2 (2J-1)} \right] -$$
$$- \frac{\mu_J}{J} m_J B - \tfrac{1}{2} \chi_{Av} B^2 - \tfrac{1}{2} \alpha_{Av} E^2 - \frac{\mu_I}{I} m_I B (1 - \sigma_{Av}) + c\, m_I m_J, \quad (3.9)$$

where $(\alpha_{//} - \alpha_{\perp})$, $(\chi_{//} - \chi_{\perp})$, $(\sigma_{//} - \sigma_{\perp})$, (μ_J/J), χ_{Av}, α_{Av}, σ_{Av} and c are respectively the coupling constants of electric polarizability, magnetic susceptibility, magnetic shielding, molecular magnetic dipole moment, magnetic susceptibility, electric polarizability, magnetic shielding, and spin-rotation interaction. The quantity μ_I is the nuclear dipole moment of the carbon nucleus. The relations between the coupling constants μ_J/J, $(\chi_{//} - \chi_{\perp})$, c, $(\sigma_{//} - \sigma_{\perp})_K$, and $(\sigma_{Av})_K$ and the diagonal tensor components from Table 3.1 are given by:

$$\begin{aligned} \mu_J/J &= G_{xx}, \\ \chi_{//} - \chi_{\perp} &= \chi_{zz} - \chi_{xx}, \\ c_K &= (M_K)_{xx}, \\ (\sigma_{//} - \sigma_{\perp})_K &= (\sigma_K)_{zz} - (\sigma_K)_{xx}, \\ (\sigma_{Av})_K &= \tfrac{1}{3}\{(\sigma_K)_{zz} + 2(\sigma_K)_{xx}\}. \end{aligned} \quad (3.10)$$

According to Eq. (3.9) the quantities χ_{Av} and α_{Av} do not depend on any quantum number. Consequently they can not be obtained from a resonance experiment.

In high magnetic fields the coupling between J and I is broken down, as has already been stated at the beginning of this section. As a consequence the quantum number m_I can not be changed in an electric dipole transition. Another result is that transitions of the type $\Delta M = \pm 1$ have to be induced (Sect. 3.5) for $O^{13}CS$, to fulfill the machine rule $\Delta m_J = \pm 1$.

It can also be seen from Eq. (3.9) that the terms in μ_{el} and $\alpha_{//} - \alpha_{\perp}$ show the same J, m_J dependence within a fixed J-state. Therefore, both quantities cannot be obtained from a single radio frequency Stark measurement. A measurement in another rotational state must be included to obtain both quantities separately.

3.4 MATRIX ELEMENTS, ENERGY LEVELS, AND COUPLING CONSTANTS OF HF AND HCl

In the calculation of the energy levels of the HF and HCl molecules the spin-spin interaction in both molecules and the chlorine quadrupole interaction in HCl have to be taken into account in addition to the interactions discussed in the previons section. The matrix elements of these interactions and the nondiagonal matrix elements of the interactions mentioned previously, are listed in the Appendix. Explicit calculations are given elsewhere (Lee 67a, Lee 70b). The coupling constants for the spin-spin interaction are d_T and d_S (Wac 67), whereas the coupling constant of the quadrupole interaction is denoted by eqQ (Wac 67).

The average susceptibility and polarizability of the HF and HCl molecules cannot be obtained from the spectra for the same reasons as for the OCS molecule. However, it is possible to evaluate the average magnetic shielding of the chlorine nucleus in HCl. The reason is that even in a high magnetic field the coupling between **J** and $\mathbf{I}_{Cl}$ is not broken as a result of the strong nuclear quadrupole interaction. Therefore, the states are not 'pure' $|Jm_J> |I_{Cl}m_{I_{Cl}}> |I_H m_{I_H}>$ -states, but linear combinations of them. If a transition of the type $\Delta M = 0$ is induced, the observable transitions (machine-rule $\Delta m_J = \pm 1$) fulfil the selection rule $\Delta m_{I_{Cl}} = \pm 1$, which makes it possible to obtain $(\sigma_{Av})_{Cl}$. The same arguments hold for the transitions of the type $\Delta M = \pm 1$ as can be shown from explicit calculations (Lee 70b).

For species with two nuclear spins different from zero it is generally not possible to obtain analytical expressions of the energy levels of the molecule using perturbation theory. For these molecules the eigenvalue problem has to be solved numerically. The matrix elements are calculated numerically with the IBM 360/50 Computer of the University, using the relationships in the Appendix and Eq. 3.9. The matrices are diagonalized using a standard library program. The output of the program provides the eigenvalues and eigenvectors of the energy matrices. The calculations are performed using 14 significant digits.

3.5 TRANSITION PROBABILITIES

The transition probability in molecular beam resonance experiments is given by the Rabi-formula (Rab 39, Ram 56, p. 119):

$$P_{p,q} = \frac{\mu_{p,q}^2 E_\sim^2}{h^2(\nu_0 - \nu)^2/4 + \mu_{p,q}^2 E_\sim^2} \sin^2\{(\omega_0 - \omega)^2/4 + 4\pi^2\mu_{p,q}^2 E_\sim^2/h^2\}^{\frac{1}{2}} t, \quad (3.11)$$

where $P_{p,q}$ gives the probability that a molecule initially in a state p is found to be in a state q after being subjected for a time t to an oscillatory field $E_\sim e^{i\omega t}$. It is assumed that p and q are different levels with energies W_p and W_q, respectively. The resonance frequency ω_0 equals $2\pi(W_p - W_q)/h$. The dipole moment matrix element between states p and q is denoted by $\mu_{p,q}$.

The eigenvector Ψ_p of the initial state p of the molecule in an external electric field E, is given by:

$$\Psi_p = \sum_{\substack{M = m_J + m_{I_1} + m_{I_2} \\ M = \text{constant}}} C_p(m_J, m_{I_1}, m_{I_2}) \mid \tilde{J} m_J > \mid I_1 m_{I_1} > \mid I_2 m_{I_2} >. \quad (3.12)$$

The constants C_p are the components of the eigenvectors of the eigenvalue problem (Sect. 3.4) and are provided by the diagonalizing procedure. The result for the dipole moment matrix element is then:

$$\mu_{p,q} = \sum_M C_p(m_J, m_{I_1}, m_{I_2})\, C_q(m_J', m_{I_1}, m_{I_2})\, \delta(m_{I_1}', m_{I_1})\, \delta(m_{I_2}', m_{I_2}) \times$$
$$\times <\tilde{J} m_J \mid \mu_{el} \mid \tilde{J} m_J'>. \quad (3.13)$$

The relevant matrix elements $<\tilde{J} m_J \mid (\mu_{el})_g \mid \tilde{J} m_J'>$ of the $J = 1$ state for $\Delta M = 0$ ($E_\sim \parallel E_{dc}$) and $\Delta M = \pm 1$ ($E_\sim \perp E_{dc}$) transitions are given by (Sch 57, Fey 68a):

$$\begin{aligned}
<\tilde{1}\ \ 0 \mid (\mu_{el})_z \mid \tilde{1}\ \ 0> &= \ \ 2R, \\
<\tilde{1} \pm 1 \mid (\mu_{el})_z \mid \tilde{1} \pm 1> &= -R, \\
<\tilde{1}\ \ 1 \mid (\mu_{el})_x \mid \tilde{1}\ \ 0> &= \ \ R, \\
<\tilde{1}\ \ 0 \mid (\mu_{el})_x \mid \tilde{1} -1> &= -R.
\end{aligned} \quad (3.14)$$

where R is a proportionality constant. Its value is unimportant as we are interested only in relative intensities.

The transition probabilities $P_{p,q}$ are calculated using Eqs. (3.11) to (3.14) and the constants C_p provided by the computer program. The sine function from Eq. (3.11) is approximated by its argument. Not all transitions with $P_{p,q} \neq 0$ are observable in a molecular beam resonance apparatus. The machine rule $\Delta m_J = \pm 1$ (Sect. 1.3) is used to determine the observable transitions.

In practice the oscillatory field is of the form $E'_{\sim}\cos\omega t$ rather than $E_{\sim}e^{i\omega t}$. As a result the resonance frequency is displaced (Sch 57, Wac 67). These shifts can be neglected in the present study.

According to Eq. (3.11), maximum intensity of a spectral line at resonance frequency ($\omega = \omega_0$) is reached if $\mu_{p,q}E_{\sim}\, t/h = 1/4$. In practice the amplitude $E_{\sim}$ is adjusted for this maximum intensity. The typical value for OCS is $E_{\sim} = 0.2$ V/cm. At higher values of E side-lines appear as can be readily calculated from

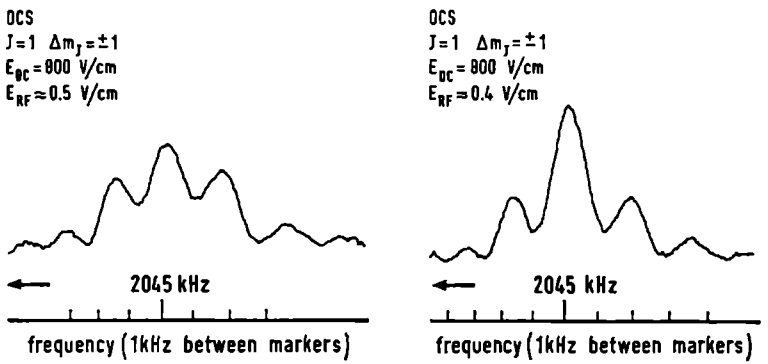

FIG. 3.1 OCS resonances two different values of the radio-frequency radiation, showing the $(\sin)^2$-property of the transition probability.

Eq. (3.11). It was possible to observe these side-lines in the present apparatus. An illustration of this phenomenon is given in Fig. 3.1. The positions of the side-lines were in agreement with the predictions (Lee 69c).

3.6 EFFECTS OF MOLECULAR VIBRATIONS

The diagonal components of the tensor operators which are given in Table 3.1 involve the coordinates of the nuclei in the molecule and both the diagonal and the off-diagonal electronic matrix elements. In the Born-Oppenheimer approximation the internuclear distance R in the molecule is treated as a parameter, and so the electronic wave functions describing the states $|\,o>$ and $|\,n>$ depend on R. Consequently the expectation values of the electronic matrix elements depend also on R. Thus, the molecular constants in Table 3.1 can be thought to be operators with respect to the vibrational states. This will generally hold for all coupling constants.

The experimental results reported in Chapt. 4 are obtained for the ground vibrational state and first excited rotational state of the molecules involved. The consequences of the effects of molecular vibration on the coupling constants are discussed in Chap. 5.

EXPERIMENTAL RESULTS

4.1 EVALUATION OF THE COUPLING CONSTANTS

The frequencies of the observed radio frequency transitions of the HF, HCl, and OCS molecules can be expressed in terms of the coupling constants. The spectra are observed in electric fields (Stark spectra) as well as in combined electric and magnetic fields (Stark-Zeeman spectra). The details of these measurements are given in the following sections.

The Stark- and Stark-Zeeman spectra of HF, HCl and OCS could be calculated to within a few kHz from coupling constants previously obtained. The unknown coupling constants $\chi_{//} - \chi_{\perp}$, $\sigma_{//} - \sigma_{\perp}$ and σ_{Av}, and if necessary, the initial coupling constants, are varied until the quantity χ^2, defined as:

$$\chi^2 = \sum_i \left(\frac{\nu_{calc}^{(i)} - \nu_{obs}^{(i)}}{\Delta \nu_i} \right)^2 \tag{4.1}$$

reaches a minimum value. Here $\nu_{calc}^{(i)}$, $\nu_{obs}^{(i)}$, and $\Delta \nu_i$ represent the frequency of the i^{th}-calculated, and observed transition and its error. The minimizing procedure is performed with a computer. The standard deviations of all of the interaction constants are calculated with the same program (Blu 68). The reported errors in the results are three times the calculated standard deviations. This is to insure a 90 % confidence limit for those results.

The general physical constants reported by Taylor *et al* (Tay 69) are used in the evaluation of the results.

4.2 CARBONYL SULPHIDE

4.2.1 *Stark spectrum*

The Stark spectra measurements on the isotopic species $^{16}O^{12}C^{32}S$, $^{16}O^{12}C^{34}S$, and $^{16}O^{13}C^{32}S$ of the carbonyl sulphide molecule are performed for the $J = 1 \rightarrow 1$, $\Delta M = \pm 1$ transitions at an electric field of 800 V/cm. The *C*-field construction with a coated slit was used in the measurements (Sect. 2.3.1). To eliminate systematic errors in the determination of the distance between the *C*-field plates, the measurements on $^{16}O^{12}C^{32}S$ were performed with two sets of

spacers of different heights, (6.3632 ± 0.0002) mm and (10.0000 ± 0.0001) mm. The Fluke 332 A Voltage Standard was calibrated with an accuracy of 3 ppm. The electric dipole moments of the isotopic species $^{16}O^{12}C^{34}S$ and $^{16}O^{13}C^{32}S$ molecules were measured relative to that of $^{16}O^{12}C^{32}S$.

The resonance frequency ν_0 of the stark transition $J = 1 \rightarrow 1$, $m_J = 0 \rightarrow \pm 1$ of the molecules $^{16}O^{12}C^{32}S$ and $^{16}O^{12}C^{34}S$ is calculated from Eq. (3.9). The result is:

$$\nu_0 = \frac{3}{20}\frac{\mu_{el}^2 E^2}{hA} - \frac{1}{5}(\alpha_{//} - \alpha_{\perp})E^2 - 0.01077\,\frac{\mu_{el}^4 E^4}{h^3 A^3}. \qquad (4.2)$$

For the molecule $^{16}O^{13}C^{32}S$ the spectral line at ν_0 is split in a doublet due to the spin-rotation interaction of the carbon nucleus $I = \frac{1}{2}$ in that molecule. As can be seen from Eq. (3.9) the splitting is equal to the absolute value of the spin-rotation coupling constant.

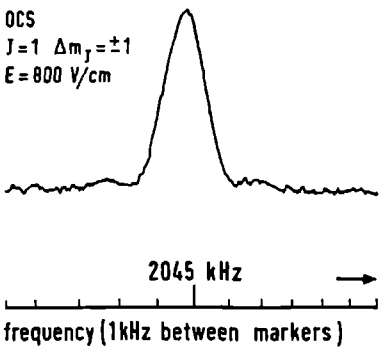

FIG. 4.1 OCS resonance.

Commercial carbonyl sulphide was used in the experiment. The measurements were performed at a source temperature of 150°K. The highest line intensity was obtained with voltages on the quadrupole rods of ± 3 kV. The voltages on the buffer fields were 1.5 kV. The half-width of the spectral lines was 650 Hz. The spectra were obtained without phase sensitive detection. A time constant of 1s and a sweep rate of 30 Hz/s was used for the $^{16}O^{12}C^{32}S$ measurements. For the measurements on the less abundant species $^{16}O^{12}C^{34}S$ (4 %) and $^{16}O^{13}C^{32}S$ (1 %) the time constant was 10 and the sweep rate 10 Hz/s. In Fig. 4.1 a recording of the $^{16}O^{12}C^{32}S$ resonance is given, showing the available sensitivity and resolution. The measured resonance frequencies are listed in Table 4.1.

TABLE 4.1 Frequencies of the observed transitions $J = 1 \rightarrow 1$, $\Delta M = \pm 1$ of isotopic species of the OCS molecule ($v = 0$). All values are in kHz.

Molecule	Stark transitions	Stark-Zeeman transitions[d]
$^{16}O^{12}C^{32}S$	1972.65 (3)[a, e]	
	2044.75 (5)[b]	
	2044.67 (4)[c]	1899.18 (5)
		2250.87 (5)
$^{16}O^{12}C^{34}S$	2097.22 (5)[c]	1955.37 (10)
		2288.76 (10)
$^{16}O^{13}C^{32}S$	2050.44 (10)[c]	1906.42 (14)
	2053.51 (10)[c]	1908.32 (14)
		2254.46 (14)
		2258.99 (14)

[a] $E = 785.762$ (44) V/cm.
[b] $E = 799.986$ (25) V/cm.
[c] $E = 800$ V/cm.
[d] E as in c, and $B = 7976.2$ (16) G.
[e] The number in parentheses gives the uncertainty in the last digit.

TABLE 4.2 Observed electric and magnetic properties of isotopic species of the OCS molecule ($v = 0$, $J = 1$).

Quantity	$^{16}O^{12}C^{32}S$	$^{16}O^{12}C^{34}S$	$^{16}O^{13}C^{32}S$	Ref.
μ_{el} (D)	0.71515 (3)			w z
	0.71525 (20)			a
	0.7124 (2)			b
μ_{el} (relative)	1.00000	1.00031 (2)	1.00017 (2)	w
g_J	−0.028839 (6)	−0.028242 (10)	−0.028710 (15)	w
	−0.02889 (2)			c
	−0.028711 (40)	−0.028127 (40)		d
$\chi_{\parallel} - \chi_{\perp}$ (kHz/kG^2)	−2.348 (3)	−2.342 (5)	−2.360 (9)	w
	−2.294 (30)	−2.339 (30)		d
	−2.09 (7)			e
c (kHz)			3.1 (2)	w
$(\sigma_{\parallel} - \sigma_{\perp})c$(ppm)			372 (42)	w

[a] References Mue 68 and Sch 70.
[b] Reference Mar 57.
[c] Reference Ced 64.
[d] Reference Fly 69.
[e] Reference Taf 68.
[w] This work.
[z] In Ref. Lee 70a another value of μ_{el} was reported as a result of using a different value of Plancks constant: $h = 6.62559\ (16) \times 10^{-34}$ J·s (*Rev. Mod. Phys.*, Oct., 1965). The present value is: $h = 6.626196\ (50) \times 10^{-34}$ J·s (Tay 69).

For the evaluation of the data we have used:
$(\alpha_{//} - \alpha_{\perp}) = (4.63 \pm 0.06) \times 10^{-24}$ cm^3 (Mue 68) and the rotational constants of Table 5.1. The results for the electric dipole moments of the isotopic species and for the spin rotation constant of the ^{13}C-nucleus in $^{16}O^{13}C^{32}S$ are given in Table 4.2. The results for the two different sets of spacers were:
$\mu_{el} = 0.71515(4)$ D (thickness : 6.3632 mm) and $\mu_{el} = 0.71516(3)$ D (thickness : 10.0000 mm). The sign of the spin-rotation constant is discussed in Chap. 5.

4.2.2 *Stark-Zeeman spectra*

The Stark-Zeeman spectra of the type $J = 1 \rightarrow 1$ and $\Delta M = \pm 1$ are obtained at an electric field of 800 V/cm and a magnetic field of about 8 kG. The transition frequencies are calculated from Eq. (3.9). Two transition frequencies are found for the spinless species and four for $^{16}O^{13}C^{32}S$. The two transitions (at frequencies ν_1 and ν_2) of the spinless species allow the determination of $\chi_{//} - \chi_{\perp}$ and the absolute value of μ_J/J. The appropriate relationships are:

$$|\mu_J/J| = \frac{|\nu_1 - \nu_2|}{2B}, \tag{4.3a}$$

and

$$\chi_{//} - \chi_{\perp} = (5/B^2)\left(\frac{\nu_1 + \nu_2}{2} - \nu_0\right). \tag{4.3b}$$

The frequency of the Stark transition at ν_0 is taken from measurements at $B = 0$. The Eqs. (4.3a) and (4.3b) can also be used for the $^{16}O^{13}C^{32}S$ molecule. The quantities ν_0, ν_1 and ν_2 then represent the average frequencies of the doublets. The measurements show that the lower frequency doublet in the Stark-Zeeman spectrum of the $^{16}O^{13}C^{32}S$ molecule is split less than the higher frequency doublet. This indicates that a certain relationship exists between c and $\sigma_{//} - \sigma_{\perp}$ as can be calculated from Eq. (3.9); namely

$$\begin{aligned} c > 0 &\longleftrightarrow (\sigma_{//} - \sigma_{\perp}) > 0, \\ \text{or } c < 0 &\longleftrightarrow (\sigma_{//} - \sigma_{\perp}) < 0. \end{aligned} \tag{4.4}$$

The splittings of the lower and higher frequency doublets are given by $|c - 4\mu_I B(\sigma_{//} - \sigma_{\perp})/5|$ and $|c + 4\mu_I B(\sigma_{//} - \sigma_{\perp})/5|$, respectively. The quantity μ_I is the magnetic dipole moment of the ^{13}C nucleus ($g_I(^{13}C) = 0.7024\ \mu_N$ (Ful 65)).

The frequencies of the measured resonances of OCS are listed in Table 4.1. The results for the magnetic susceptibility anisotropy and the magnetic dipole moments of the three isotopic species, together with the results for the spin-

rotation constant and the magnetic shielding anisotropy of ^{13}C in $^{16}O^{13}C^{32}S$, are given in Table 4.2. The sign of $\chi_{//} - \chi_{\perp}$ follows directly from Eq. (4.3b). It should be noted that the sign of μ_J can not be obtained directly from these measurements. However, in chapter 5 a discussion is given of the sign of the magnetic dipole moment, of the magnetic shielding anisotropy of ^{13}C, and of the spin-rotation constant in OCS.

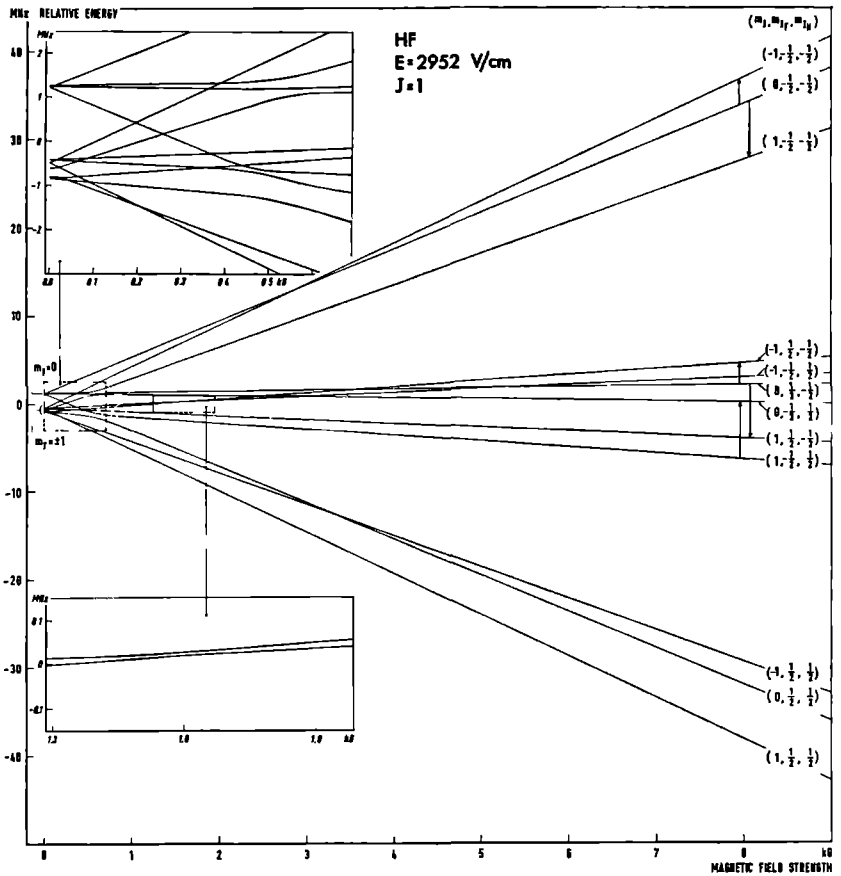

FIG. 4.2 Energy level diagram of HF.

4.3 HYDROGEN FLUORIDE

4.3.1 *Introduction*

Because of the large magnetic moments of the hydrogen and fluorine nuclei ($\mu_H = 2.79278\ \mu_N$, $\mu_F = 2.6287\ \mu_N$ (Ful 65)) the Zeeman effect for these nuclei

is rather strong at high magnetic fields. With both spins parallel in a field of 500 G the Zeeman effect is already 2 MHz. This is comparable to the Stark energy at an electric field of 3 kV/cm.

We have calculated the energy levels of the HF molecule in the $J = 1$ rotational state in parallel electric and magnetic fields. The electric field was 3 kV/cm and the magnetic field was varied between zero and 9 kG. A repulsion of states was found at approximately 500 G for states with $M = 0$ and $M = 1$ and at 1500 G for states with $M = -1$. The energy level diagram is given in Fig. 4.2.

It was found that five transition frequencies were observable. In molecules where the repulsion of states does not occur the number of observable transitions is eight (Dre 61). This loss of spectral lines was not expected at the start of this work. Therefore it was not practical to study this phenomenon as the apparatus was not designed for it. Fortunately it was well possible to determine the magnetic coupling constants from the spectrum. The observed transitions are also given in Fig. 4.2.

4.3.2 *Stark-Zeeman spectrum*

The measurements on HF have been performed on the $J = 1 \rightarrow 1, \Delta M = \pm 1$ transitions at a magnetic field of 8414.6 (17) G and an electric field of about 1500 V/cm. The *C*-field construction with the aluminium-gold film and with uncoated slit was used. The shifts in line positions due to the uncoated slit were included in the unperturbed Stark transition frequency ν_0. This was done because we were interested primarily in magnetic effects.

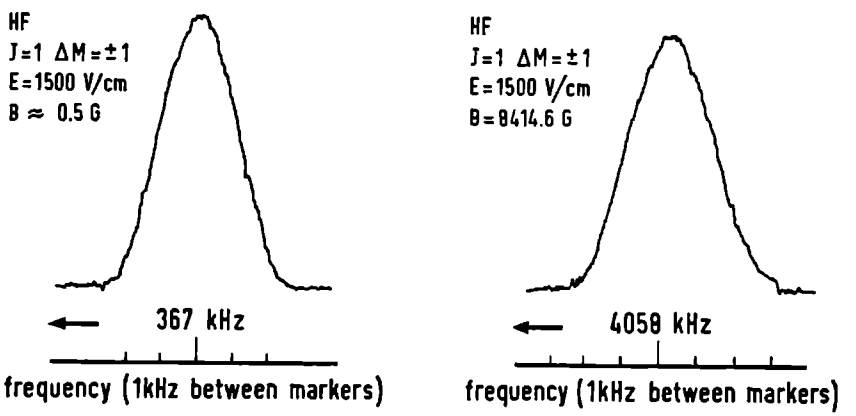

FIG. 4.3 HF resonance at nearly zero and high magnetic field.

Commercial hydrogen fluoride was used in the experiment. The measurements were performed with a teflon source. The voltages on the quadrupole rods were adjusted for optimum line intensity ($\pm$ 12 kV). The voltages applied to the buffer fields were 4 kV. The half-widths of the spectral lines were 1.3 kHz. The spectra were obtained without phase sensitive detection. The time constant was 1s. The spectral lines were recorded at a sweep rate of 30 Hz/s. In Fig. 4.3 recordings of an observed Stark transition and Stark-Zeeman transition are given. The measured Stark-Zeeman transition frequencies and two transition frequencies at nearly zero (< 0.5 G) magnetic field are listed in Table 4.3. The latter frequencies are used to determine the relative value of the Stark effect. Such a measurement is necessary as $\chi_{//} - \chi_{\perp}$, μ_{el} and $\alpha_{//} - \alpha_{\perp}$ depend in the same way on the external fields as can be seen from Eq. (3.9). So an uncertainty in μ_{el} also gives an uncertainty in $\chi_{//} - \chi_{\perp}$.

TABLE 4.3 Frequencies of the observed transition $J = 1 \rightarrow 1$, $\Delta M = \pm 1$ of the HF molecule ($v = 0$). All values are in kHz.

Stark transitions[a]		Stark-Zeeman transitions[b]	
Observed Frequency	Deviation (Calc.-Obs.)	Observed Frequency	Deviation (Calc.-Obs.)
367.02 (3)	—0.04	4057.92 (5)	0.00
829.52 (3)	0.05	4452.29 (5)	—0.01
		5067.42 (5)	0.01
		5288.87 (5)	—0.01
		5444.33 (5)	—0.01

[a] $E = 1500$V/cm.
[b] E as in a, and $B = 8414.6$ (17) G.

In the evaluation of the data we have used the following constants: $c_F = 307.637$ kHz, $c_H = -71.128$ kHz, $d_T = 28.675$ kHz, $d_S = 0.529$ kHz (Mue 70), and $A = 616361$ MHz (Web 68). The results for the magnetic dipole moment, the magnetic susceptibility anisotropy and the magnetic shielding anisotropy at the hydrogen and the fluorine nuclei can be found in Table 4.4.

TABLE 4.4 Observed magnetic properties of the HF molecule ($v = 0$, $J = 1$).

Quantity	This work	Baker *et al* (Bak 61)
g_J	0.74104 (15)	0.7392 (5)
$\chi_{//} - \chi_{\perp}$ (kHz/kG^2)	0.132 (6)	
$(\sigma_{//} - \sigma_{\perp})_F$(ppm)	108 (9)	
$(\sigma_{//} - \sigma_{\perp})_H$(ppm)	24 (9)	

4.4.1 *Introduction*

The strong quadrupole interaction of the chlorine nucleus in HCl ($eqQ \approx -67$ MHz) splits the $J = 1$ rotational level into 3 sublevels. The hyperfine interaction of the hydrogen nucleus and the external Stark- and Zeeman fields splits these sublevels even further.

We have calculated the energy level diagram of the HCl molecule in constant external electric field and magnetic field varying from zero to 9 kG. It was found that at magnetic fields between 2 and 8 kG, certain states will repell each other. The energy level diagram is given in Fig. 4.4. This repulsion of states influenced, as in the experiment of HF, the number of observable lines. However, the loss in the number of observable lines was not serious.

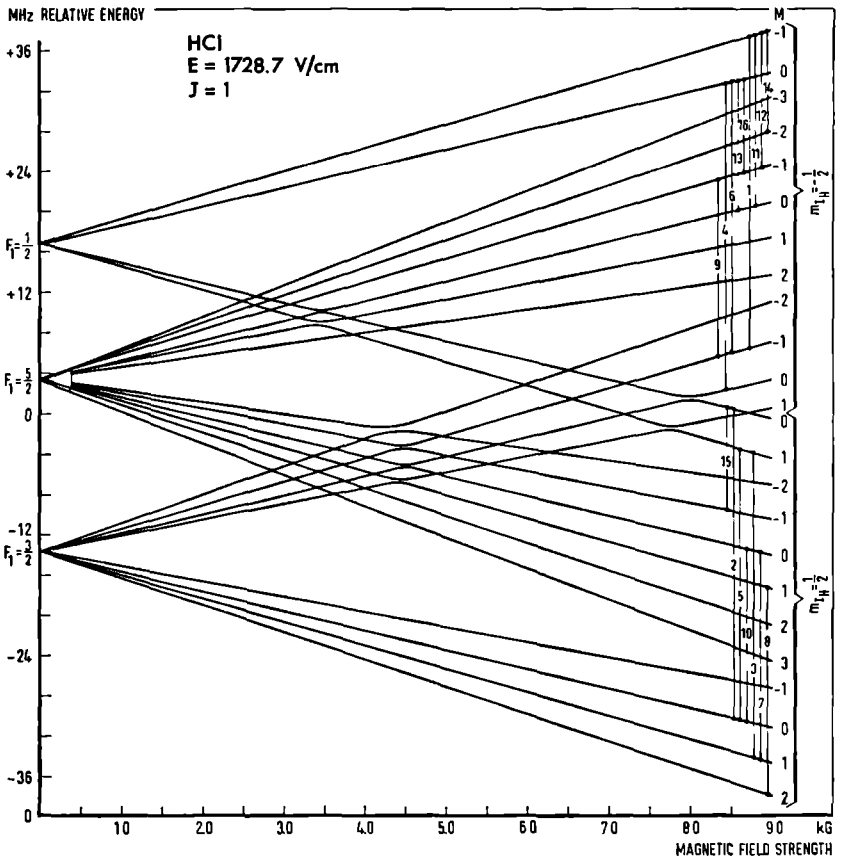

FIG. 4.4 Energy level diagram of $H^{35}Cl$.

The measurements on $H^{35}Cl$ were performed on the $J = 1 \rightarrow 1, \Delta M = 0, \pm 1$ transitions at electric field of 1728.69 V/cm and a magnetic field of 8411.9 G. We searched for all transitions at those fields which give good signal to noise ratio and good resolution; sixteen lines were found.

The *C*-field construction with aluminium-gold film and uncoated slit was used. The slit was located 3 mm to one side of the beam axis in order to reduce the influence of the uncated slit on the line position. Each experimental line was measured for both polarities of the voltage to the *C*-field. The final transition frequency was defined as the average value of the two results. Each run was carried out at least twice in order to minimize uncertainty in the results.

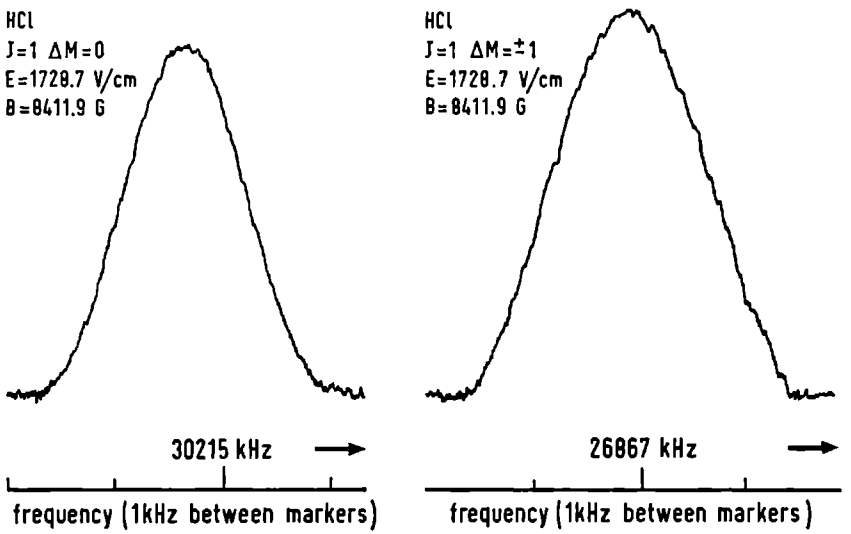

FIG. 4.5 HCl resonances at high magnetic field of the type $\Delta M = 0$ and $\Delta M = \pm 1$.

Commercial hydrogen chloride was used in the experiments. The measurements were performed at a source temperature of 300° K. The voltages on the quadrupole rods were $\pm$ 12 kV. The voltages on the buffer fields were 4 kV. The half-widths of the spectral lines were 0.7 kHz for the $\Delta M = 0$ transitions and 0.9 kHz for the $\Delta M = \pm 1$ transitions. Time constants up to 3s were used in the measurements. The spectral lines were recorded at sweep rates between 10 and 30 Hz/s. In Fig. 4.5 recordings of a $\Delta M = 0$ transition and of a $\Delta M = \pm 1$ transition are given. The line at 26867 kHz possess a strong Zeeman effect and was measured regularly to monitor the fluctuation in the magnetic field

during the measurements. This makes it possible to correct the results for a drift in the field during the measurements. The line at 30215 kHz was also measured regularly. This was done to monitor the fluctuation in the electric field. During the experiments the fluctuation in that field was less than 2×10^{-5}. Measurements in nearly zero magnetic field were performed to determine the Stark effect of the molecule. As outlined in Sect. 4.3, the Stark effect has to be known accurately for a correct evaluation of the magnetic susceptibility anisotropy.

TABLE 4.5 Frequencies of the observed transitions $J = 1 \rightarrow 1$, $\Delta M = 0, \pm 1$ of the $H^{35}Cl$ molecule ($v = 0$). All values are in kHz.

Stark-transitions[a]		Stark-Zeeman transitions[b]	
Observed frequency	Deviation (Calc.-Obs.)	Observed frequency	Deviation (Calc.-Obs.)
16958.814 (20)	0.034	9602.288 (30)	—0.009
16947.730 (20)	—0.037	10268.439 (20)	—0.009
		10307.188 (20)	0.004
		12886.577 (20)	0.009
		13501.397 (20)	—0.012
		16785.708 (20)	—0.016
		17261.103 (10)	—0.012
		17264.372 (10)	0.001
		20445.076 (20)	—0.002
		20625.419 (20)	0.021
		26866.667 (20)	—0.016
		26870.947 (20)	0.028
		30214.553 (10)	—0.003
		30235.326 (10)	—0.001
		30739.059 (10)	0.007
		30765.757 (10)	0.001

[a] $E = 1728.7$ V/cm.
[b] E as in a and $B = 8411.9$ (17) G.

The measured transition frequencies are listed in Table 4.5. The reported frequencies are corrected for the second order perturbation of the type $(eqQ)^2/A$ (Tow 55, p. 517). In the evaluation of the data we have used $A = 312990$ MHz (Ran 65), μ_{Cl} (^{35}Cl) $= 0.82183\ \mu_N$ (Ful 65), and $\alpha_{//} - \alpha_{\perp} = 0.31$ Å^3 (Bri 66, Kai 70). The hyperfine coupling constants determined by Kaiser (Kai 70) are used as the initial set. The results for the hyperfine coupling constants, the electric dipole moment, the rotational magnetic moment, the magnetic susceptibility anisotropy, the magnetic shielding anisotropy at the hydrogen and at the chlorine nuclei, and the average value of the magnetic shielding of the chlorine nucleus are given in Table 4.6.

TABLE 4.6 Observed electric and magnetic properties of the $H^{35}Cl$ molecule ($v = 0, J = 1$).

Quantity		This work		Kaiser (Kai 70)	
μ_{el}	(D)	1.1086	(3)	1.108	(5)
$eq\ Q_{Cl}$	(kHz)	−67618.81	(15)	−67618.93	(47)
c_{Cl}	(kHz)	53.841	(18)	53.851	(42)
c_H	(kHz)	− 41.70	(8)	− 41.80	(25)
d_T	(kHz)	5.59	(6)	5.585	
d_S	(kHz)	0.02	(6)	0.00	
g_J		0.45935	(9)	0.47	(3)
$\chi_{//} - \chi_\perp$	(kHz/kG^2)	− 0.048	(18)		
$(\sigma_{//} - \sigma_\perp)_{Cl}$	(ppm)	300	(24)		
$(\sigma_{//} - \sigma_\perp)_H$	(ppm)	21	(5)		
$(\sigma_{Av})_{Cl}$	(ppm)	740	(200)		

INTERPRETATION AND DISCUSSION OF THE RESULTS

5.1 INTRODUCTION

In this chapter the coupling constants obtained from the experiments on HF, HCl and OCS are analyzed. The direct results of these analyses are: the electronic contributions to the rotational magnetic dipole moments, the paramagnetic susceptibilities, the sign of the electric dipole moment in OCS, the diamagnetic susceptibility anisotropies, the molecular quadrupole moments, and the diamagnetic shielding anisotropies. These quantities, together with the coupling constants already obtained in Chap. 4, will be compared with results from other investigations, like microwave Zeeman-spectroscopy, MBMR spectroscopy and line-broadening experiments.

Sect. 5.6 is devoted to a discussion of the accuracy of the determination of the dipole moment of the OCS molecule. In the same section a method is suggested to obtain a more accurate value of the rotational magnetic dipole moment of the HCl molecule. Basically, a method is presented in which the value of the rotational magnetic moment of the HCl molecule is related to the magnetic moment of the chlorine nucleus.

Theoretical calculations of electric and magnetic properties for the electronic ground state of the hydrogen fluoride and hydrogen chloride molecules have been performed recently by several authors, using various choices of the LCAO-MO-SCF wave functions (Cad 66, Cad 67a, Cad 67b, Ben 69). In order to test the accuracy of the resulting charge distributions the values of several electric and magnetic properties obtained from the present experiments are compared with results of these calculations. Only a few calculations are available for the carbonyl sulphide molecule. The present results may therefore serve as a guide for future calculations.

All coupling constants were obtained for the ground vibrational state ($v = 0$) and first excited rotational state ($J = 1$) of the molecules involved. As was already stated in Sect. 3.6, the coupling constants may be thought to be as operators with respect to the vibrational states. Therefore the effect of molecular vibrations on these coupling constants and the effect of the vibrations on the evaluation of quantities, like molecular quadrupole moment, from the observed coupling constants are investigated in the next section.

For a $^1\Sigma$-diatomic molecule the average value for vibration-rotation state vJ, of an arbitrary operator $\mathbf{O}$ which is a known function of internuclear distance R may be expanded about the equilibrium distance R_e as:

$$<\mathbf{O}>_{vJ} = O_e + O_e' R_e <\xi>_{vJ} + \tfrac{1}{2} O_e'' R_e^2 <\xi>_{vJ} + \ldots \qquad (5.1)$$

The primed quantities are the successive derivatives of the operator $\mathbf{O}$ with respect to R at internuclear equilibrium distance R_e, and $\xi = (R - R_e)/R_e$. With Dunhams rotation-vibration theory (Tow 55, p. 9), the average of ξ^n is expressible in powers of A_e/ω_e, the ratio of the rotational constant to the vibration frequency of the molecule, and the Dunham potential constants a_i (Ram 56, p. 230, Sch 61). The constants A_e, ω_e, R_e and a_1 are for nearly all simple molecules known from rotation and vibration spectra. If terms through order $(A_e/\omega_e)^2$ are retained, the following equation is obtained for the expectation value $<\mathbf{O}>_{vJ}$ of an arbitrary operator $\mathbf{O}$.

$$\begin{aligned}
<\mathbf{O}>_{vJ} = {} & O_e + (A_e/\omega_e)^2 \{O_e' R_e (-\tfrac{15}{4} a_3 + \tfrac{23}{4} a_1 a_2 - \tfrac{21}{8} a_1^3) \\
& + O_e'' R_e^2 (-\tfrac{3}{4} a_2 + \tfrac{7}{8} a_1^2) - \tfrac{7}{24} a_1 O_e''' R_e^3 + \tfrac{1}{16} O_e'''' R_e^4\} \\
& + (A_e/\omega_e)(v + \tfrac{1}{2}) \{O_e' R_e (-3a_1) + O_e'' R_e^2\} \\
& + (A_e/\omega_e)^2 (v + \tfrac{1}{2})^2 \{O_e' R_e (-15a_3 + 39 a_1 a_2 - \tfrac{45}{2} a_1^3) \\
& + \tfrac{1}{2} O_e'' R_e^2 (-6a_2 + 15 a_1^2) - \tfrac{15}{6} a_1 O_e''' R_e^3 + \tfrac{1}{4} O_e'''' R_e^4\} \\
& + 4 (A_e/\omega_e)^2 J (J + 1) O_e' R_e. \qquad (5.2)
\end{aligned}$$

The diatomic molecules which have been studied in this thesis have A_e/ω_e-values which are less than 5×10^{-3}. Consequently, for the ground vibrational state of the molecule, it is probably sufficient to retain only terms through order (A_e/ω_e) in Eq. (5.2). The dependence on R of some of the coupling constants and molecular constants is not known, however, and so the quality of this approximation is difficult to assess.

The validity of this approximation was checked for the ground vibrational state of HCl by calculating the expectation values of R^n with $-3 < n < 4$, and comparing the results with accurate results obtained by Kaiser (Kai 70). It was found that the accuracy of the approximate results was good for negative n-values and deviated by 0.3 % at $n = 4$.

In the analysis of results from hydrogen experiments (Bar 54, Qui 58) it was assumed that the molecular constants could be written as a constant times R^n. It was found empirically that the highest value of n was 3.8 (Qui 58), which

occurred for the paramagnetic contribution to the magnetic susceptibility. An empirical value of n in HF or HCl is not available. There is, however, a calculation of the paramagnetic susceptibility of HF (Ste 64) from which n can be evaluated. It was found that $n = 4.3$ for this quantity (Lee 70b). It is therefore assumed that the first order approximation, which retains only the term through order A_e/ω_e in Eq. 5.2, is correct for HCl to within 0.3 %.

Because $(A_e/\omega_e)_{HF}/(A_e/\omega_e)_{HCl} = 1.5$ (Table 5.1), it is assumed that the accuracy of the approximation for HF is correct to within 0.5 %.

The theory of vibrations of triatomic linear molecules is very complicated (Tow 55, Chapt. 2, Mor 67). Consequently, the internuclear distances in the OCS molecule, evaluated from different rotation spectra, are only known to within 10^{-3} (Mor 67). Because of the rotation-vibration interaction in the OCS molecule, the rotational constant for the ground vibrational state is decreased by 0.3 % with respect to its value at equilibrium separations of the nuclei. The R-dependency of the rotational constant is R^{-2}. The vibrational influence on the expectation value of a molecular quantity with R^n-dependency is, in first order, proportional to the exponant n. It may therefore be assumed that the vibrational influence on a quantity in OCS with R^4-dependency is 0.6 %.

In the expressions for G^e_{xx} and $(M_K)^e_{xx}$ in Table 3.1 the rotational constant A is multiplied by an off-diagonal electronic matrix element. As will be shown in the following sections the quantities G^e_{xx} and $(M_K)^e_{xx}$ can be obtained from experiments in the ground vibrational state of the molecule. For a correct evaluation of the off-diagonal electronic matrix elements, it is necessary to take into account the influence of the molecular vibrations. This is achieved by the relation

$$<\mathbf{O}_1\mathbf{O}_2>_{vJ} - <\mathbf{O}_1>_{vJ}<\mathbf{O}_2>_{vJ} = (A_e/\omega_e)\,(v + \tfrac{1}{2})\,(2O'_{1e}\,O'_{2e}\,R_e^2), \qquad (5.3)$$

where $\mathbf{O}_1 = A$ and $\mathbf{O}_2$ is one of the off-diagonal electronic matrix elements.

TABLE 5.1 Molecular constants of HF, $H^{35}Cl$, $^{16}O^{12}C^{32}S$, $^{16}O^{12}C^{34}S$ and $^{16}O^{13}C^{32}S$.

Quantity		HF[a]	HCl[b]	OCS[c]		
r_e	(Å)	0.91681 (2)	1.2746	O-C: 1.157 (2) C-S: 1.560 (2)		
		$H^{19}F$[a]	$H^{35}Cl$[b]	$^{16}O^{12}C^{32}S$[d]	$^{16}O^{12}C^{34}S$[d]	$^{16}O^{13}C^{32}S$[d]
A_e	(cm^{-1})	20.9557 (9)	10.5934			
ω_e	(cm^{-1})	4138.32 (6)	2990.94			
A_0	(MHz)	616361 (6)	312991	6081.49	5932.82	6061.89
a_1		−2.2537	−2.3645			

[a] Reference Web 68, [b] Reference Ram 65, [c] Reference Mor 67, [d] Reference Tow 55.

The first order derivatives in Eq. (5.3) have to be obtained experimentally or theoretically. An experimental determination is possible, as can be seen from Eq. (5.2) if the expectation value $<\mathbf{O}>_{vJ}$ is observed for two J values within a vibrational state. This method was used for HCl to obtain the first order derivative of the paramagnetic contribution in the magnetic shielding.

5.3 THE ROTATIONAL MAGNETIC DIPOLE MOMENTS

5.3.1 *Determination of the electronic contribution to the rotational magnetic dipole moments*

The rotational magnetic dipole moment μ_J/J can be expressed as a sum of a nuclear and an electronic contribution as can be seen from Eq. (3.10) and Table 3.1. The nuclear contributions, $(\mu_J/J)^n$, can be calculated from the molecular structure (Table 5.1). For a $^1\Sigma$-diatomic molecule, with nuclei with masses m_1 and m_2 and nuclear charges Z_1e and Z_2e, respectively, the expression $(\mu_J/J)^n$ can be reduced to:

$$(\mu_J/J)^n = \frac{eh}{4\pi m_{red}} Z_{eff}, \tag{5.4}$$

with

$$Z_{eff} = Z_1 \left(\frac{m_2}{m_1 + m_2} \right)^2 + Z_2 \left(\frac{m_1}{m_1 + m_2} \right)^2, \tag{5.5}$$

and

$$m_{red} = m_1 m_2/(m_1 + m_2).$$

According to Eq. (5.4) the value of $(\mu_J/J)^n$ does not depend on the rotational and vibrational states of the diatomic molecule. This property is essentially due to the fact that the vibrational motions of the nuclei have no components in the direction of their rotational velocities. Vibrational motions in the directions of the rotational velocities are allowed, however, for linear triatomic molecules. If these motions are neglected an equation similar to Eq. (5.4) can then be derived for the triatomic molecules. By using the definition of the rotational constant A (Tow 55, p. 10), and the experimental evidence that the masses of the nuclei ^{16}O, ^{12}C, ^{32}S divided by the proton mass are equal to the number of nucleons in that nuclei divided by 0.5040 (Mat 65), it is found that

$$(\mu_J/J)^n = 0.5040(3)\ \mu_N, \tag{5.6}$$

for the $^{16}O^{12}C^{32}S$ molecule. The uncertainty in the constant appearing in

Eq. (5.6) arises from the different mass defects of the nuclei in the $^{16}O^{12}C^{32}S$ molecule. The influence of the molecular vibrations on the result of Eq. (5.6) cannot be estimated. Therefore no additional error has been introduced in that equation. We have supposed that the rotational magnetic dipole moment of OCS in the ground vibrational state equals the value given in Eq. (5.6).

TABLE 5.2 Nuclear and electronic parts of the rotational magnetic dipole moments of HF, $H^{35}Cl$ and OCS. All values in μ_N.

Quantity	HF	$H^{35}Cl$	$^{16}O^{12}C^{32}S$
$<(\mu_J/J)^n>_{v=0}$	0.97367	0.98571	0.5040 (3)
$<(\mu_J/J)^e>_{v=0}$	—0.23263 (15)	—0.52636 (9)	—0.5328 (3)

The nuclear contributions to the magnetic moments of HF and HCl are calculated from Eq. (5.4) using the 1964 Mass Table of Mattauch *et al* (Mat 65). The results are given in Table 5.2. The moments $(\mu_J/J)^n$ of $^{16}O^{12}C^{34}S$ and $^{16}O^{13}C^{32}S$ are not considered.

From these calculated values of $(\mu_J/J)^n$, and the experimental results for (μ_J/J) (Chap. 4), the values of the electronic contribution to the moments, $(\mu_J/J)^e$, of HF and HCl are calculated. These results are also given in Table 5.2.

5.3.2. *Determination of the average paramagnetic susceptibilities*

The average paramagnetic susceptibility of a $^1\Sigma$-diatomic molecule is given by:

$$\chi^p_{Av} = \tfrac{1}{3}(2\chi_{xx} + \chi_{zz})^p. \tag{5.7}$$

With the definitions of the components of the χ-tensor (Table 3.1) this gives:

$$\chi^p_{Av} = \tfrac{4}{3}\mu_B^2\,(L, L), \tag{5.7a}$$

where

$$(L, L) = \sum_{n \neq o} \frac{|<o \mid L_x \mid n>|^2}{E_n - E_o} \tag{5.8}$$

The matrix element (L, L) is calculated from $(\mu_J/J)^e$ using the relation (Table 3.1):

$$(\mu_J/J)^e = -4\,\mu_B A\,(L, L). \tag{5.9}$$

The effects of the molecular vibration are taken into account by using Eq. (5.3) with $A \quad \mathbf{O}_1$ and $(L, L) \cdot \mathbf{O}_2$. The first derivative of (L, L) in HF was cal-

culated from a theoretical investigation by Stevens *et al* (Ste 64, Lee 70b). The first derivative of (L, L) in HCl is unknown. Application of Eq. (5.3) increases the value of (L, L) by 4.4 % with respect to its value if the right side of Eq. (5.3) is taken equal to zero. If the quantity (L, L) in HCl is proportional to R^4, with R the internuclear distance, than it is readily seen from Eq. (5.3) that the effects of molecular vibration will increase the quantity (L, L) in HCl by 3 % over its value obtained from Eq. (5.10). The vibrational influences on the determination of χ^{p}_{Av} for the OCS molecule are not considered. The results for χ^{p}_{Av} for HF, HCl, and OCS are given in Table 5.3.

TABLE 5.3 Average paramagnetic susceptibilities and diamagnetic susceptibility anisotropies of HF, $H^{35}Cl$ and OCS. All values in 10^{-6}erg/G^2 ·mole.

Quantity	HF	$H^{35}Cl$	$^{16}O^{12}C^{32}S$
$<\chi^{p}_{Av}>_{v=0}$	0.5579 (4)	2.46 (5)	127 (3)
$<(\chi_{\parallel} - \chi_{\perp})^{d}>_{v=0}$	1.342 (25)	3.49 (10)	181 (4)

5.3.3 *Determination of the sign of the electric dipole moment of the OCS molecule*

It was first shown by Townes *et al* (Tow 55a) that the sign of the electric dipole moment of a molecule can be obtained from the isotopic dependence of the rotational magnetic dipole moment. The appropriate equation is:

$$\frac{h(\mu_J/J)_2}{2\pi A_2} - \frac{h(\mu_J/J)_1}{2\pi A_1} = 2 \mid \mu_{el} \mid \delta \qquad (5.10)$$

The quantities $(\mu_J/J)_1$, A_1, $(\mu_J/J)_2$ and A_2 are the rotational magnetic dipole moment and the rotational constant of two different isotopic species of the OCS molecule. If we assume that the internuclear distances are the same in both isotopes then the quantity δ is the coordinate of the center of mass of isotopic 1 referred to the center of mass of isotope 2. In the case of OCS the direction of a positive δ is from oxygen to sulfur.

Using the magnetic dipole moments of Table 4.2 Eq. (5.10) gives:

$$\mid \mu_{el} \mid = (0.64 \pm 0.06) \text{ D},$$

and the polarity (—) O C S (+).

5.4.1 *Determination of the diamagnetic susceptibility anisotropies*

The diamagnetic susceptibility anisotropy of a $^1\Sigma$-diatomic molecule is given by (Eq. 3.10, Table 3.1):

$$(\chi_{//} - \chi_{\perp})^{d} = \frac{e^2}{4m} <o \mid \tfrac{1}{2}\Sigma_i (3z_i^2 - r_i^2) \mid o>. \tag{5.11}$$

The quantity $(\chi_{//} - \chi_{\perp})^{d}$ is obtained from the experimental value of the total magnetic susceptibility anisotropy $(\chi_{//} - \chi_{\perp})$, the paramagnetic part $(\chi_{//} - \chi_{\perp})^{p} = -\frac{3}{2}\chi^{p}_{Av}$, and the calculated value of the nuclear contribution $(\chi_{//} - \chi_{\perp})^{n}$. The expectation value of $(\chi_{//} - \chi_{\perp})^{n}$ for HF and HCl is less than 10^{-8} erg/G^2· mole and is neglected. The value of $(\chi_{//} - \chi_{\perp})^{n}$ for OCS is 10^{-7}erg/G^2· mole. The results for $(\chi_{//} - \chi_{\perp})^{d}$ for HF, HCl, and OCS are given in Table 5.3.

5.4.2 *Determination of the molecular quadrupole moments*

The electric quadrupole moment Θ of a molecule is the sum of a nuclear contribution Θ^{n}, and an electronic contribution Θ^{e}. The nuclear part in the molecular quadrupole moment of a linear molecule is given by:

$$\Theta^{n} = e\Sigma_K Z_K r_K^2, \tag{5.12}$$

the electronic part is:

$$\Theta^{e} = e<o \mid \tfrac{1}{2}\Sigma_i (3z_i^2 - r_i^2) \mid o>. \tag{5.13}$$

Comparison of Eqs. (5.11) and (5.13) shows that the quantities Θ^{e} and $(\chi_{//} - \chi_{\perp})^{d}$ are proportional to each other (Ram 50). So, the electronic contribution to the molecular quadrupole moment can be readily calculated from the observed diamagnetic shielding anisotropy. The expectation values of Θ^{n} for the ground vibrational state of HF and HCl are calculated using Eq. (5.2) in which the terms through order A_e/ω_e are retained. The quantity Θ^{n} of OCS is calculated for the equilibrium distances in the molecule. The results for Θ^{e}, Θ^{n}, and Θ are given in Table 5.4.

TABLE 5.4 Molecular quadrupole moments of HF, $H^{35}Cl$, and OCS. All values are in 10^{-26} esu · cm^2.

Quantity	HF	$H^{35}Cl$	$^{16}O^{12}C^{32}S$	$^{16}O^{12}C^{34}S$	$^{16}O^{13}C^{32}S$	Reference
$<\Theta^e>_{v=0}$	—1.52 (3)	—3.95 (8)	—21.2 (4)			w
$<\Theta^n>_{v=0}$	3.88	7.69	20.4 (4)			w
$<\Theta>_{v=0}$	2.36 (3)	3.74 (8)	— 0.786 (14)	—0.858 (23)	—0.716 (40)	w
	3	3.75 (50)				a
			— 0.88 (15)			b
			— 2.10			c
			| 1 (1) |			d
			| 2.79 (20) |			e

[a] Reference Ben 63.
[b] Reference Fly 69.
[c] Reference Taf 68.
[d] Reference Ber 68.
[e] Reference Mur 68.
[w] This work.

It can be seen from Table 5.4 that the electronic and nuclear contributions to the molecular quadrupole moment of OCS cancel each other. Therefore the molecular quadrupole moment of OCS is calculated directly from Eq. (3.10) and Table 3.1 by eliminating the quantity (L, L). The appropriate relation is:

$$\Theta = -\frac{4m}{e}(\chi_{//} - \chi_{\perp}) + \frac{h\,\mu_J}{2\pi AJ} + me\sum_K \frac{Z_K r_K^2}{m_K}. \tag{5.14}$$

The last term contributes 0.034×10^{-26}esu·cm^2 to the molecular quadrupole moment. The results of Θ for the three isotopic species of OCS are given in Table 5.4.

We must note that Eq. (5.14) is only valid if molecular quantities at equilibrium distance are substituted in that equation. These quantities are however not obtained in an experiment. By substituting the molecular quantities for the ground vibrational state in Eq. (5.14), errors of 2–5 per cent are introduced for systems like HF, HCl, and OCS.

5.5 THE MAGNETIC SHIELDING

5.5.1 *Determination of the diamagnetic shielding anisotropies and average chlorine diamagnetic shielding in* $H^{35}Cl$

From the definition of $(\sigma_{//} - \sigma_{\perp})_K^d$ (Eq. (3.10), Table 3.1) one can see that this quantity can be obtained from the experimental values of the spin-rotation

constant and the magnetic shielding anisotropy. The method for the evaluation of $(\sigma_{//} - \sigma_{\perp})^{d}_{K}$ is very similar to the method for the evaluation of the diamagnetic susceptibility anisotropy from the rotational magnetic dipole moment and the anisotropy in the magnetic susceptibility.

The electronic contribution to the spin-rotation constant, c^{e}_{K}, is first calculated from the observed spin-rotation constant and the calculated value of the nuclear contribution to the spin-rotation constant. The paramagnetic shielding anisotropy is then calculated from c^{e}_{K} using the relation:

$$c^{e}_{K} = \frac{2\,\mu_N g_K A}{\mu_B} (\sigma_{//} - \sigma_{\perp})^{p}_{K}. \tag{5.15}$$

Here the effects of the molecular vibrations are included by using Eq. (5.3) with $A = \mathbf{O}_1$ and (Q, Q') $\mathbf{O}_2$, where the quantity (Q, Q'), defined as:

$$(Q, Q') = \sum_{n \neq o} | \langle o | Q_x | n \rangle \langle n | Q'_x | o \rangle + \text{c.c.} | / (E_n - E_o), \tag{5.16}$$

is that appearing in the expression

$$(\sigma_{//} - \sigma_{\perp})^{p}_{K} = \frac{\mu_o \mu_B^2}{2\pi} (Q, Q'). \tag{5.17}$$

The diamagnetic shielding anisotropy is finally calculated from the observed shielding anisotropy, and the paramagnetic shielding anisotropy obtained from Eq. (5.17).

The first derivative of the quantity (Q, Q') at the chlorine nucleus is calculated from the present experimental result for c_{Cl} and the result for c_{Cl} at $J = 2$ obtained by Kaiser (Kai 70), using Eq. (5.2). Application of Eq. (5.3) increased (Q, Q') by 1.6 % with respect to its value when Eq. (5.15) was applied directly.

The results for $(\sigma_{//} - \sigma_{\perp})^{p}_{Cl}$ and $(\sigma_{//} - \sigma_{\perp})^{d}_{Cl}$ are:

$$(\sigma_{//} - \sigma_{\perp})^{p}_{Cl} = 304\ (5)\ \text{ppm},$$
$$(\sigma_{//} - \sigma_{\perp})^{d}_{Cl} = -4\ (25)\ \text{ppm}.$$

The average paramagnetic shielding at the chlorine nucleus is obtained using the relation:

$$(\sigma_{Av})^{p}_{Cl} = -\tfrac{2}{3} (\sigma_{//} - \sigma_{\perp})^{p}_{Cl}. \tag{5.18}$$

Inserting the value of $(\sigma_{//} - \sigma_{\perp})^{p}_{Cl}$ in Eq. (5.18) gives:

$$(\sigma_{Av})^{p}_{Cl} = -202\ (4)\ \text{ppm}.$$

From the observed value of $(\sigma_{Av})_{Cl}$ and the value of $(\sigma_{Av})^{p}_{Cl}$ obtained above we find that

$$(\sigma_{Av})^{d}_{Cl} = 942\ (200)\ \text{ppm}.$$

The first derivative of (Q, Q') at the hydrogen nucleus could not be obtained from the results of Kaiser (Kai 70). An estimated correction of 2 % is applied to the result for $(\sigma_{//} - \sigma_{\perp})^{p}_{H}$. The result for the paramagnetic shielding anisotropy is then:

$$(\sigma_{//} - \sigma_{\perp})^{p}_{H} = 169\ (5)\ \text{ppm}.$$

From the experimental value of $(\sigma_{//} - \sigma_{\perp})_{H}$ we get

$$(\sigma_{//} - \sigma_{\perp})^{d}_{H} = -148\ (7)\ \text{ppm}.$$

5.5.2 *Determination of the diamagnetic shielding anisotropies in HF*

The diamagnetic shielding anisotropies in HF are calculated using the same method as given in the preceeding section. The vibrational correction are taken from the paper by Hindermann and Cornwell (Hin 68). These authors calculated the paramagnetic shielding anisotropies at the hydrogen and fluorine nuclei from the measurements of Weiss (Wei 63):

$$(\sigma_{//} - \sigma_{\perp})^{p}_{H} = 119.6\ (5)\ \text{ppm},$$
$$(\sigma_{//} - \sigma_{\perp})^{p}_{F} = 108.6\ (5)\ \text{ppm}.$$

Comparison with the experimental value of $(\sigma_{//} - \sigma_{\perp})_{H}$ and $(\sigma_{//} - \sigma_{\perp})_{F}$ yields:

$$(\sigma_{//} - \sigma_{\perp})^{d}_{H} = -96\ (9)\ \text{ppm},$$
$$(\sigma_{//} - \sigma_{\perp})^{d}_{F} = -1\ (9)\ \text{ppm}.$$

5.5.3 *Determination of the carbon diamagnetic shielding anisotropy and the sign of the spin-rotation constant in* $O^{13}CS$

From the spectra it was only possible to determine that the spin-rotation constant and the magnetic shielding anisotropy of the carbon nucleus have the

same signs (Sect. 4.2.2). To obtain the signs the method of Flygare and Goodisman (Fly 68) was used. These authors found that for a linear molecule the following relation holds:

$$(\sigma_{Av})_K = (\sigma_{Av})_K^d \textit{ (free atom)} - \frac{\mu_B}{\mu_N} \frac{c_K}{2g_K A}, \qquad (5.19)$$

where $(\sigma_{Av})_K^d$ *(free atom)* is the average diamagnetic shielding of the free atom. With $(\sigma_{Av})_K^d$ *(free atom)* = 261 ppm (Ram 56, p. 177) and the c-constant from Table 4.2 this gives the two values $(\sigma_{Av})_K = (261 \pm 222$ ppm). The positive sign holds for a negative c-constant and the negative sign for a positive c-constant. There is no experimental or theoretical value for σ_{Av} in carbonyl sulphide. However, there does exist a calculation by Stevens (see Lip 66) for carbon monoxide. The result is $\sigma_{Av} = 11.5$ ppm. So the most probable choice for carbonyl sulphide is $\sigma_{Av} = 39$ ppm. This gives a positive c-constant and a positive $(\sigma_{//} - \sigma_{\perp})$ for ^{13}C in OCS.

From the c-constant the paramagnetic part of $(\sigma_{//} - \sigma_{\perp})$ is calculated (Sect. 5.5.1).

$$(\sigma_{//} - \sigma_{\perp})_C^p = 579\ (21) \text{ ppm}.$$

From this quantity and the experimental result for $(\sigma_{//} - \sigma_{\perp})_C$ it follows that:

$$(\sigma_{//} - \sigma_{\perp})_C^d = -207\ (42) \text{ ppm}.$$

5.6 THE ACCURACY OF THE ELECTRIC DIPOLE MOMENT AND MAGNETIC DIPOLE MOMENT DETERMINATIONS

5.6.1 *The electric dipole moment of OCS*

The value for the electric dipole moment of OCS obtained from the measurements reported in Sect. 4.2.1 was reproducible within the indicated error limits when the C-field condenser was reassembled and when the polarity of the voltage on the C-field plates was changed. The estimated inaccuracies in the parameters used in the evaluation of the electric dipole moment were:

voltage to the C-field plates:	3.2 ppm,
thickness spacers (6.3632 mm):	32 ppm,
unperfect optical contact between spacers and C-field plates:	46 ppm,
resonance frequency:	16 ppm.

The inaccuracies in the polarizability anisotropy (Mue 68), Plancks constant (Tay 69), and the rotational constant (Tow 55) are much lower than the inaccuracies given above, and are not considered further. From the estimated inaccuracies it can be seen that that of the electric field determination gives the highest contribution to the uncertainty in the electric dipole moment. To get a better feeling for the estimated uncertainty in the unperfect optical contact between spacers and *C*-field plates measurements were performed with two sets of spacers with different thickness. The resulting values for the electric dipole moments were in excellent agreement with each other and it was concluded that the estimated uncertainty in the electric field determination was quite reasonable.

The electric dipole moment is evaluated using Eq. 4.2. The result should be corrected, however, for the vibrational motion of the molecule, as was done in the evaluation of the paramagnetic susceptibility (Sect. 5.3.2). Since no measurements in other rotational or vibrational states of the OCS molecule were performed, the influence of the vibrational motion on the determination of the electric dipole moment could not be estimated. The true value of the electric dipole moment in the ground vibrational state will differ slightly from the result given in Table 4.2.[1] However, when the present value is substituted in Eq.(4.2) together with the rotational constant for the ground vibrational state, the precise value of the frequency of the Stark transition $J = 1 \rightarrow 1$, $m_J = 0 \rightarrow \pm 1$ is obtained. In this manner the electric field strength in another MBER spectrometer can be calibrated.

The present experiment provides the most precise determination of the electric dipole moment of any molecule to date. The result can be used as a standard to calibrate MBER spectrometers and conventional Stark spectrometers.

5.6.2 *The rotational magnetic dipole moment of HCl*

The accuracy of the present results of the rotational magnetic dipole moments of the molecules OCS, HF and HCl is determined by the accuracy of the determination of the external magnetic field. As discussed in Sect. 2.7 this accuracy was 2×10^{-4}. However, the experiment on HCl provides a possibility of calibrating the field and obtaining a more accurate value for the rotational magnetic dipole moment of the HCl molecule.

From the measured $H^{35}Cl$ Stark-Zeeman spectrum, and the known values of the external magnetic field B and the magnetic moment of the chlorine

[1] The effect of the vibrational motion of the OCS molecule on the dipole moment determination of this molecule is probably of the order of 10^{-3}.

nucleus, the rotational magnetic dipole moment μ_J/J and the average magnetic shielding $(\sigma_{Av})_{Cl}$ are obtained (Sect. 4.4.2, Table 4.6). It is found, however, that the values of μ_J/J, $(\sigma_{Av})_{Cl}$ and B are correlated strongly, but not with the remaining coupling constants. This means that the substitution of another B-value in the computer program provides other values of μ_J/J and $(\sigma_{Av})_{Cl}$. Results obtained for μ_J/J and $(\sigma_{Av})_{Cl}$ at three values of B are given in column 2 and 3 of Table 5.5. The reported errors originate from the uncertainties in the determination of the resonance frequencies.

TABLE 5.5 Data analysis results for μ_J/J, $(\sigma_{Av})_{Cl}$ and $(\sigma_{Av})^d_{Cl}$ of $H^{35}Cl$ ($v = 0$, $J = 1$) at three different values of the substituted magnetic field in the computer[a].

B (G)	(μ_J/J) (μ_N)	$(\sigma_{Av})_{Cl}$ (ppm)	$(\sigma_{Av})^d_{Cl}$ (ppm)
8410.9	0.459409 (7)	619 (8)	821 (8)
8411.9	0.459355 (7)	740 (8)	942 (8)
8412.9	0.459300 (7)	857 (8)	1059 (8)

[a] The following value is used for the magnetic dipole moment of the chlorine nucleus: $\mu_{Cl} = 0.82183\ (5)\ \mu_N$ (Ful 65).

From the obtained values of the average magnetic shielding constants (column 3 of Table 5.5) the average diamagnetic shielding constants $(\sigma_{Av})^d_{Cl}$ are calculated using the method described in Sect. 5.5.1. The results are given in the column 4 of Table 5.5. From the results in Table 5.5, the values of the magnetic field and the rotational magnetic dipole moment can than be evaluated, with the theoretical value of the quantity $(\sigma_{Av})^d_{Cl}$ (1150 ppm) being used as a standard. The result for μ_J/J obtained from this method is:

$$\mu_J/J = 0.45926\ (3)\ \mu_N,$$

where the accuracy of μ_J/J is determined by the accuracy of the magnetic dipole moment of the chlorine nucleus.

The result reported in Chapt. 4 ($\mu_J/J = 0.45935\ \mu_N$) differs by 2×10^{-4} from the result obtained in this section. This indicates that the estimated accuracy of the determination of the magnetic field was quite reasonable.

5.7 DISCUSSIONS AND COMPARISONS WITH RESULTS OF OTHER INVESTIGATORS

5.7.1 *Nuclear hyperfine coupling constants*

The results for the nuclear hyperfine coupling constants of $H^{35}Cl$ agree very well with the results obtained by Kaiser (Kai 70, Table 4.6). Of these constants,

the spin-spin interaction constant d_S is the smallest. Also in the present experiment the value of this constant is not significantly different from zero.

The spin-rotation coupling constant c of ^{13}C in OCS is found to be positive. Consequently, the electronic contribution to c is positive. The positive electronic contribution to c is also predicted by a simplified localized orbital theory (Fly 64a, Lee 66, p. 28).

5.7.2 *Electric dipole moments*

An accurate determination of the electric dipole moment of OCS was performed in 1957 by Marshall and Weber (Mar 57). Their value: $\mu_{el} = 0.7124$ D has since then been generally accepted for the calibration of Stark cells used for dipole moment measurements on other molecules. In 1968, however, Muenter (Mue 68) reported a significantly different value: $\mu_{el} = 0.71521\ (20)$ D obtained by the MBER method.[2] The present result confirms Muenters value.

The result for the electric dipole moment of $H^{35}Cl$ is in good agreement with the result obtained by Kaiser (Kai 70, Table 4.6).

5.7.3 *Rotational magnetic dipole moments*

The rotational magnetic dipole moments of OCS and HF have been measured previously by the MBMR method (OCS: Ced 64; HF: Bak 61). The results for both molecules are, however, not in agreement with the present results. The discrepancies can be explained from the state selection properties of the MBMR method. A systematic error in the field determination can be probably disregarded because the absolute value of the OCS moment from the MBMR method is larger than the moment from the MBER method, whereas for HF the situation is reversed.

In the MBMR method the molecules are selected as to m_J and not as to J. The most highly populated J-states for HF and HCl are the $J = 3$ state and the $J = 20$ state, respectively. Consequently, the rotational magnetic dipole moment, obtained from a measurement with the MBMR method, will show a shift due to the centrifugal distorsion of the molecule. This can be seen as follows.

It was shown in Sect. 5.3.2 that the quantity (L, L) of HF has an R^4-dependence, and so the quantity $(\mu_J/J)^e$ will have an R^2-dependence (Table 3.1). By

---

[2] In his paper Muenter (Mue 68) used an incorrect value for Plancks constant. The corrected dipole moment value of Muenter is: $\mu_{el} = 0.71525\ (20)$ D (Sch 70).

using Eq. (5.2) it is then readily seen that the change $\Delta\,(\mu_J/J)^e$ in $(\mu_J/J)^e$ with respect to its value for $J = 1$, is given by:

$$\Delta\,(\mu_J/J)^e = 8(A_e/\omega_e)^2\ \ \{J(J+1) - 2\}\ \ (\mu_J/J)^e. \qquad (5.20)$$

By using Eq. (5.20), $J = 3$, $A_e/\omega_e = 5 \times 10^{-3}$, and $(\mu_J/J)^e$ from Table 5.2 we obtain:

$$\Delta\,(\mu_J/J)^e = -0.0008\ \mu_N.$$

Consequently, the moment evaluated with the MBMR method will be 0.0008 μ_N lower than the moment evaluated with the MBER method, because the magnetic dipole moment of HF is positive. The calculated shift in (μ_J/J) is in rather good agreement with the observed shift in (μ_J/J) between the result from the MBER method and the result from the MBMR method.

Basically, the same calculation can be done for the OCS molecule. However, for this linear triatomic molecule a relation like Eq. (5.2) does not exist. We assume however that this equation is valid for this molecule. The typical value for A_e/ω_e of the OCS molecule will be about 5×10^{-4}. By using Eq. (5.20), $J = 20$, and $(\mu_J/J)^e$ from Table 5.2 we find:

$$\Delta\,(\mu_J/J)^e = -0.0004\ \mu_N.$$

As the magnetic moment of the OCS molecule is negative the absolute value will be increased by 0.0004 μ_N. The calculated shift in (μ_J/J) is roughly in agreement with the observed shift in (μ_J/J).

We have made many assumptions in the calculations given above and so the good agreement may be accidental. One may state, however, that at least the signs of the discrepancies between the results obtained from both methods can be explained from Eq. (5.20).

The rotational magnetic dipole moment of the OCS molecule has also been determined by Flygare *et al* (Fly 69) with a Zeeman microwave spectrometer. His result does not agree with the present result (Table 4.2). The most probable reason would be a systematic error in the magnetic field determination; the internal consistency of the present results and the results of Flygare *et al* is perfect, as can be seen from isotopic substitution effects. A systematic error in our field determination is unlikely.

5.7.4 *Molecular quadrupole moments*

The molecular quadrupole moment Θ of the OCS molecule has been determined recently by several investigators, the results showing a considerable

spread. When this work was in progress (Lee 69a), Flygare *et al* (Fly 69) reported a determination of Θ using a conventional absorption spectrometer equipped with high field magnet. These authors determined Θ from the measured anisotropy in the magnetic susceptibility of the OCS molecule. The result, $\Theta = -0.88\ (15) \times 10^{-26}$esu·cm^2, was in agreement with our preliminary determination of Θ (Lee 69a) but was in sharp disagreement with the determination of Θ by Taft and Daily (Taf 68, $\Theta = -2.10$), using the same method as Flygare *et al.* The result of Flygare *el al* was also in strong disagreement with the determination from line broadening by Murphy and Boggs (Mur 68, $|\Theta| = 2.79\ (20)$), but it was well within limits set by Berendts and Dymanus $|\Theta| = 1\ (1)$ (Ber 68). This was quite surprising because Berendts and Dymanus used the original Anderson theory with a rather questionable matching procedure to interpret their experimental data, while Murphy and Boggs used an improved theory. Flygare *et al* discussed the possibility that the quadrupole moment active in line broadening has its origin not at the molecular center of mass. However, they found that if the large values of $\pm$ 2.79 are compared to the center of mass results, the $\pm$ 2.79 moments must have their origins at points beyond the nuclei in the molecule. This is clearly unreasonable.

The molecular quadrupole moment in OCS is also reported by Buckingham *et al* (Buc 68, $\Theta = -0.3\ (1) \times 10^{-26}$esu·cm^2). Their experiments do not refer to the molecular center of mass (cm) as origin, but to the so-called "effective quadrupole center". Flygare *et al* have calculated that the "effective quadrupole center" is between the carbon and sulfur atom, at approximately 0.1 Å from the carbon atom.

The present results confirm the good agreement found between the results obtained by Flygare *et al* (Fly 69) and our preliminary determination of Θ (Lee 69a). The disagreement with the result of Taft and Dailey (Taf 68) is a direct consequence of a serious deviation between the values of $(\chi_{//} - \chi_{\perp})$ obtained by Taft and Daily on the one side and by Flygare *et al* and by us on the other.

In the present work the molecular quadrupole moments of two other isotopic species of the OCS molecule are also obtained. The value of the molecular quadrupole moment of a polar molecule depends on the choice of origin of the system in which the moment is defined. This is described by the relation:

$$\Theta_2 - \Theta_1 = 2\ |\ \mu_{el}\ |\ \delta, \tag{5.21}$$

where Θ_1 and Θ_2 are the quadrupole moments defined with respect to the origin of system 1 and 2, respectively. The quantities μ_{el} and δ are defined in Sect. 5.3.3. Using Eq. (5.21) and Table 5.4 the quadrupole moments with

respect to cm of the $^{16}O^{12}C^{32}S$ molecule are calculated (in 10^{-26}esu·cm^2):

$$\Theta\,(^{16}O^{12}C^{32}S) = -0.786\ (14),$$
$$\Theta\,(^{16}O^{12}C^{34}S) = -0.810\ (23),$$
$$\Theta\,(^{16}O^{13}C^{32}S) = -0.728\ (40).$$

The results are in good agreement with each other, particularly the results for the most abundant species. The conclusion is that the determination of molecular quadrupole moments from measurements of diamagnetic susceptibility anisotropies (Ram 50) is reliable. A similar conclusion was already drawn from the experiments on the hydrogen molecule (Bar 54, Qui 58).

The average value of the quadrupole moments of the three isotopic species of OCS, defined with respect to the molecular center of mass of the $^{16}O^{12}C^{32}S$ molecule, is

$$\Theta = -0.787\ (12) \times 10^{-26}\text{esu}\cdot\text{cm}^2.$$

The effect of the vibrations of the OCS molecule on the validity of Eq. (5.14) cannot be easily estimated. These effects may be quite large as Θ is the difference of two quantities which nearly cancels each other.[3] It may be assumed that the vibrational influence on the value of each quantity appearing in Eq. (5.14) is of the order of 0.3 % (Sect. 5.2). Consequently, the effect of the molecular vibration on the determination of Θ of the OCS molecule, using Eq. (5.14), can be of the order of 5 %. This means that the error limits in the result for Θ mentioned above have to be increased. If these greater error limits are taken into account, the result for the quadrupole moment of the OCS molecule is:

$$\Theta = -0.79\ (4) \times 10^{-26}\text{esu}\cdot\text{cm}^2.$$

The molecular quadrupole moments of the HF and HCl molecules in the ground vibrational state are obtained in this work to within a few per cent. The moments were obtained previously by Benedict and Herman (Ben 63) using Anderson theory of collision broadening. It was only possible to estimate a

[3] The magnitudes of the quantities in Eq. (5.14) are about:

$$-\frac{4m}{e}(\chi_{//} - \chi_{\perp}) = 3.54 \times 10^{-39}\ \text{C}\cdot\text{m}^2,$$

and $$\frac{h\mu_J}{2\pi AJ} = -3.81 \times 10^{-39}\ \text{C}\cdot\text{m}^2.$$

rough value for the molecular quadrupole moment of HF ($\Theta \approx 3$) from their experiments. The result for the HCl molecule was more accurate: $\Theta = 3.75\,(50)$. Both values are in agreement with the present results. It should be remarked, however, that the nuclear contribution to the molecular quadrupole moment of HF and HCl is quite strong and is only partly compensated by the electronic contribution to the moment. Line-broadening theories are probably more reliable for strong quadrupole moments.

As already stated the quadrupole moments of HF and HCl are obtained in the present experiment for the ground vibrational state of the molecules, whereas theoretical calculations of this quantity (Sect. 5.8) have been performed at the equilibrium distance in the molecule. It is not possible to evaluate from the present results, the results for the equilibrium distance without any loss of accuracy. The simplest approach is to calculate the nuclear contribution for the equilibrium distance in the molecule and to leave the electronic contribution unchanged, but with the introduction of an additional error of $(-3a_1 + 1)$ $(A_e/\omega_e) \times 100\,\%)$[4]. The additional errors in Θ^e are then 4 % for HF and 3 % for HCl. The resulting quadrupole moments are:

$$\Theta_{eq}\,(\mathrm{HF}) = 2.21\,(7) \times 10^{-26}\mathrm{esu\cdot cm^2},$$
$$\Theta_{eq}\,(\mathrm{HCl}) = 3.53\,(14) \times 10^{-26}\mathrm{esu\cdot cm^2}.$$

The results will be compared with theoretical results in Sect. (5.8).

5.7.5 *Diamagnetic shielding*

In the present work the diamagnetic shielding anisotropies of the nuclei with nonzero spin in HF, $H^{35}Cl$ and $O^{13}CS$ have been obtained as well as the average diamagnetic shielding of the chlorine nucleus in $H^{35}Cl$ (Sect. 5.5). All these properties have been determined experimentally for the first time.

It was shown by Flygare and Goodisman (Fly 68) that the average diamagnetic shielding $(\sigma_{Av})^d_K$ at nucleus K can be evaluated from the relation:

$$(\sigma_{Av})^d_K = (\sigma_{Av})^d_K\ (\textit{free atom}) + \tfrac{1}{3}\frac{e^2\mu_o}{4\pi m}\sum_{L\neq K}\frac{Z_L}{r_{LK}} \qquad (5.22)$$

The authors compared the result from Eq. (5.22) with results from theoretical

[4] The error $(-3a_1 + 1)$ (A_e/ω_e) is obtained as follows. It is assumed that the electronic contribution in Θ has an R^2— dependence. Substitution of this assumed property of Θ^e in Eq. (5.2) gives the stated result.

calculations for a number of molecules. It turned out that Eq. (5.22) gives reliable estimates (to within 1 ppm) for the average diamagnetic shielding at a nucleus in a molecule. The validity of Eq. (5.22) is related to the isoelectric principle; the negligeable change in dissociation energy with change in nuclear charge (total electrons and internuclear distance are kept constant), as discussed by Flygare *et al* (Fly 68). It is clear that the quantity $(\sigma_{Av})^d_K$ cannot be used as a critical test of theoretical calculations, as it is insensitive to the wave function and can already be calculated with the simple expression given above.

It was also attempted by Flygare *et al* to compute the individual diagonal components of the diamagnetic shielding tensors in molecules by a directional variation of Eq. (5.22). From their results a relation for the anisotropy in the diamagnetic shielding is calculated:

$$(\sigma_{//} - \sigma_{\perp})^d_K = -\frac{e^2\mu_o}{8\pi m} \sum_{L \neq K} \frac{Z_L}{r_{LK}}. \tag{5.23}$$

Substituting of the relevant constants in Eq. (5.23) gives the following results:

$$\begin{aligned}
(\sigma_{//} - \sigma_{\perp})^d_H \text{ (in HF)} &= -137 \text{ ppm}, \\
(\sigma_{//} - \sigma_{\perp})^d_F \text{ (in HF)} &= -\ 15 \text{ ppm}, \\
(\sigma_{//} - \sigma_{\perp})^d_H \text{ (in } H^{35}Cl) &= -186 \text{ ppm}, \\
(\sigma_{//} - \sigma_{\perp})^d_{Cl} \text{ (in } H^{35}Cl) &= -\ 11 \text{ ppm}, \\
\text{and} \quad (\sigma_{//} - \sigma_{\perp})^d_C \text{ (in } O^{13}CS) &= -240 \text{ ppm}.
\end{aligned}$$

The anisotropies at the fluorine, chlorine and carbon nuclei show rather good agreement with the experimental values (Sect. 5.5). The calculated results at the hydrogen nuclei in HF and HCl show, however, a significant deviation from the experimental results. Consequently, the approach of Flygare *et al* for the calculation of general diamagnetic shielding anisotropies is too simple.

The average diamagnetic shielding at the chlorine nucleus in HCl shows rather good agreement with the theoretical result $(\sigma_{Av})^d_{Cl}$ (theoretical) = 1150 ppm (Rot 70)). The quantity has been used in Sect. 5.6 for the calibration of the external magnetic field.

5.8 COMPARISON OF EXPERIMENTAL RESULTS OF HF AND HCl WITH RESULTS FROM AB-INITIO CALCULATIONS

5.8.1 *Review of recent ab-inito calculations*

The hydrogen fluoride and hydrogen chloride molecules are often used as test cases for molecular calculations. The most extensive calculations have been

performed by Cade and Huo, who determined Hartree-Fock wavefunctions for the ground states of the first row and the second row hydrides (Cad 67a, Cad 67b; extensive bibligraphies of past calculations are included in their papers). The wavefunctions obtained by Cade and Huo are the self-consistent-field wavefunctions obtained from the solutions of the Hartree-Fock-Roothaan (HFR) equations. Large sets of Slater-type functions centered on both nuclei were used as the expansion basis, and extensive optimization of the orbital exponents has been carried out. The calculation yielded the spectroscopic constants A_e, α_e, ω_e, $\omega_e x_e$, R_e, and k_e (Cad 67a, Table 17; Cad 67b, Table 16). The fractional errors for R_e, A_e and ω_e were considerably smaller than corresponding errors previously calculated for other molecules. The authors concluded that the diatomic hydrides are apparently much less sensitive to the deterioration of the form of the Hartree-Fock wavefunction at large R-values. This was further indicated by the fact that for the first time reasonable $\omega_e x_e$ values were predicted, although the fractional error was not comfortably small.

Because of the importance of the work of Cade and Huo, McLean and Yoshimine (McL 67) decided to repeat the calculations using a computer program able to work with larger basis sets. In addition they calculated a wide variety of molecular properties with Cade and Huo's wavefunctions and with wavefunctions expanded in a larger basis set. In their calculations they used HF and HCl as test cases. The results of McLean and Yoshimine confirmed the accuracy of Cade and Huo's work. For both molecules there was a close agreement for all computed properties using the Cade and Huo and McLean and Yoshimine basis sets, with the exception of the parallel component of the molecular electric polarizability.

Recently, Bender and Davidson (Ben 69) reported ab-initio calculations of molecular properties of the first-row hydrides using accurate configuration-interaction wavefunctions. The groundstate functions were constructed from approximate natural orbitals. The wavefunctions give properties, such as the electric dipole moment, more accurately than did the SCF wavefunctions. According to the authors, the increased accuracy was brought about by including single as well as double excitations even though they contributed very little to the energy.

In the theoretical investigations of Cade *et al*, McLean *et al* and Bender *et al* various ground state properties are calculated. Second order properties of HF, like paramagnetic susceptibility and paramagnetic nuclear shielding, are calculated by Stevens and Lipscomb (Ste 64) using perturbed Hartree-Fock theory. The results of their calculations for the rotational magnetic moment, the spin-rotation constant of the hydrogen and fluorine nuclei and the average shielding of the hydrogen nucleus showed rather good agreement with the experimental

results. The result for the average susceptibility disagreed with the experimental result from a liquidphase measurement (Ste 64), but is in good agreement with the theoretical results recently published by other investigators (McL 67, Ben 69).

5.8.2 *Comparison of observed and calculated electric and magnetic properties of HF and HCl*

The ab-initio calculations of McLean *et al* (McL 67) and Bender *et al* (Ben 69) have provided theoretical values of the total energy, the electric dipole moment, and molecular quadrupole moment of the HF and HCl molecules.

Their results are listed in Table 5.6 and 5.7 along with the experimental results and the theoretical results obtained by Stevens and Lipscomb (Ste 64).

It is readily seen from Table 5.6 that the quadrupole moment of the HF molecule as calculated by Bender and Davidson is in good agreement with the observed value. So for the HF molecule, the calculated electric dipole moment as well as the calculated molecular quadrupole moment show good agreement (within 3 %) with the observed values. This has not been the case untill now, with any polar molecule. The calculated results for μ_{el} and Θ of McLean and Yoshimine are about 6–8 % higher than the observed values.

The calculated results for the paramagnetic susceptibility and the rotational magnetic moment are in rather good agreement with the observed values, as already stated in the previous section.

The calculated values obtained by McLean *et al* and Cade *et al* for the electric dipole and molecular quadrupole moments of the HCl molecule are approximately 6–10 % higher than the observed values. The same discrepancy was also found with the same type of calculations on the HF molecule.

5.9 CONCLUSIONS

This investigation has proved that the molecular-beam electric-resonance method provides an excellent capability of obtaining accurate values of electric as well as magnetic properties of molecules like HF, HCl, and OCS. It has shown that the molecular quadrupole moment of HF can be calculated accurately from approximate naturel orbitals; untill now this was proved only for the electric dipole moment.

The internal consistency of the experimental results has been checked by measurements on three isotopic species of OCS. The electric dipole moment obtained from the isotopic dependence of the magnetic moment is in good agreement with the Stark result, and the quadrupole moments for the three isotopic species agree as well.

TABLE 5.6 Calculated and observed electric and magnetic properties of the HF molecule. All results are reported for equilibrium internuclear distance (1.7328 a.u.), unless otherwise specified.

Quantity		Calculated				Observed	Reference
		Stevens *et al*[a]	Cade *et al*[b]	McLean *et al*[b]	Bender *et al*[c]		
Total energy	(a.u.)	−100.045	−100.070	−100.070	−100.356	−100.530	d
Diamagnetic shielding							
$(\sigma_{Av})_F^d$	(ppm)	481.6	482.2	482.2	482.1		
$(\sigma_{Av})_H^d$	(ppm)	108.4	108.5	108.5	108.5	108.9±0.8	e
Diamagnetic shielding anisotropy							
$(\sigma_{//} - \sigma_{\perp})_F^d$	(ppm)					−1±9	w, x
$(\sigma_{//} - \sigma_{\perp})_H^d$	(ppm)					−96±9	w, x
Paramagnetic susceptibility							
$\chi^P{}_{Av}$	(10^{-6} erg/G^2 · mole)	0.64[x]				0.5579	w, x
Diamagnetic susceptibility anisotropy							
$(\chi_{//} - \chi_{\perp})^d$	(10^{-6} erg/G^2 · mole)		1.222	1.244		1.342±0.025	w, x
Electric dipole moment							
μ_{el}	(D)		1.941	1.934	1.816	1.7965	f
Molecular quadrupole moment							
Θ	(10^{-26} esu · cm^2)		2.35	2.33	2.20	2.21±0.07	w
Rotational magnetic moment							
μ_J/J	(μ_N)	0.738[x]				0.74104±0.00015	w
Electric polarizability anisotropy							
$(\alpha_{//} - \alpha_{\perp})$	(Å^3)	0.236					

[a] Reference Ste 64.
[b] Reference McL 67.
[c] Reference Ben 69.
[d] Reference Cad 67a.
[e] Reference Hin 68.
[f] Reference Mue 70.
[w] This work.
[x] Result for the ground vibrational state.

TABLE 5.7 Calculated and observed electric and magnetic properties of the $H^{35}Cl$ molecule. All results are reported for equilibrium internuclear distance (2.4085 a.u), unless otherwise specified.

Quantity		Calculated		Observed	Reference
		Cade *et al*[a]	McLean *et al*[a]		
Total energy	(a.u.)	−460 110	−460.110	−462.148	[b]
Diamagnetic shielding					
$(\sigma_{Av})^{d}_{Cl}$	(ppm)	1150.3	1150.3		
$(\sigma_{Av})^{d}_{H}$	(ppm)	141.8	141 9		
Diamagnetic shielding anisotropy					
$(\sigma_{//} - \sigma_{\perp})_{Cl}$	(ppm)			−4 ± 25	w, x
$(\sigma_{//} - \sigma_{\perp})^{d}_{H}$	(ppm)			−148 ± 7	w, x
Paramagnetic susceptibility					
$\chi^{p}{}_{Av}$	(10^{-6} erg/G^2 · mole)			2 46	w, x
Diamagnetic susceptibility anisotropy					
$(\chi_{//} - \chi_{\perp})^{d}$	(10^{-6} erg/G^2 · mole)			3.49	w, x
Electric dipole moment					
μ_{el}	(D)	1.196	1 215	1.0933 ± 0.0005	[c]
Molecular quadrupole moment					
Θ	(10^{-26} esu · cm^2)	3 80	3.74	3.53 ± 0.14	w
Rotational magnetic moment					
μ_J/J	(μ_N)			0 45926 ± 0.00003	w, x
Electric polarizability anisotropy					
$(\alpha_{//} - \alpha_{\perp})$	(Å^3)			0 31	[d]
Nuclear quadrupole coupling constant					
eqQ	(MHz)	−66.4	−66 5	−66.80 ± 0.01	[c]

[a] Reference McL 67.
[b] Reference Cad 67b.
[c] Reference Kai 70.
[d] Reference Bri 66.
[w] This work.
[x] Result for the ground vibrational state.

The line broadening data of HF and HCl show rather good agreement with the present beam results. This is probably because of the rather high values of the moments.

The diamagnetic shielding anisotropies are obtained rather accurately, but there exist no calculations for these properties. The simple theory of Flygare and Goodisman is not powerful enough to explain them.

In the analysis of the observed coupling constants of HF and HCl it became clear that the molecular vibrations cannot be neglected. The influence of the molecular vibration on the evaluation of the electric and magnetic properties are taken into account as far as possible in the present investigation. However, results from measurements on other vibrational states will improve the final results. These measurements can be performed with the present apparatus.

Keeping in mind the high precision of the present investigation it is hoped that the theoreticians will provide also electric and magnetic properties in the ground vibrational state of a molecule. This will improve the knowledge about these properties, and make it possible to compare these calculated results directly with experiment.

$$< m_J m_I \mid \mathbf{I} \cdot (1 - \sigma) \cdot \mathbf{B} \mid m_J' m_I' > = B m_I \delta(m_J', m_J)\, \delta(m_I', m_I) \left[1 - \sigma_{Av} + \right.$$

$$\left. + 2\, \frac{3m_J^2 - J(J+1)}{3(2J+3)(2J-1)} (\sigma_{//} - \sigma_\perp) \right] (\pm)\, (\tfrac{1}{2})\, B\, (\sigma_{//} - \sigma_\perp)\, \delta(m_I', m_I \mp 1) \times$$

$$\times\, \delta(m_J', m_J \pm 1) \times \frac{(\pm)\, 2m_J + 1}{(2J+3)(2J-1)} \sqrt{I(I+1) - m_I(m_I \mp 1)} \times$$

$$\times \sqrt{J(J+1) - m_J(m_J \pm 1)},$$

$$c < m_J\, m_I \mid \mathbf{I} \cdot \mathbf{J} \mid m_J'\, m_I' > = c\, [\delta(m_J', m_J)\, \delta(m_I', m_I)\, m_J\, m_I +$$

$$+ \tfrac{1}{2}\, \delta(m_I', m_I \pm 1)\, \delta(m_J', m_J \mp 1) \sqrt{I(I-1) - m_I(m_I \pm 1)} \times$$

$$\times \sqrt{J(J+1) - m_J(m_J \mp 1)}],$$

$$< m_J\, m_I\, m_G \mid \mathbf{I} \cdot \mathbf{d} \cdot \mathbf{G} \mid m_J'\, m_I'\, m_G' > = \delta(m_J', m_J) \left\{ m_I\, m_G\, \delta(m_I', m_I) \times \right.$$

$$\times\, \delta(m_G', m_G) \left\{ d_S + 2\, \frac{3m_J^2 - J(J+1)}{(2J+3)(2J-1)} d_T \right\} - \tfrac{1}{2}\, \delta(m_I', m_I \pm 1)\, \delta(m_G', m_G \mp 1) \times$$

$$\times \sqrt{I(I+1) - m_I(m_I \pm 1)} \sqrt{G(G+1) - m_G(m_G \mp 1)} \times$$

$$\times \left\{ - d_S + \frac{3m_J^2 - J(J+1)}{(2J+3)(2J-1)} d_T \right\} \left. \right\} (\pm)\, \tfrac{3}{2}\, d_T\, \delta(m_J', m_J \pm 1) \left\{ \delta(m_I', m_I) \times \right.$$

$$\times\, \delta(m_G', m_G \mp 1)\, m_I \sqrt{G(G+1) - m_G(m_G \mp 1)} + \delta(m_G', m_G) \times$$

$$\left. \times\, \delta(m_J', m_I \mp 1)\, m_G \sqrt{I(I+1) - m_I(m_I \mp 1)} \right\} \sqrt{J(J+1) - m_J(m_J \pm 1)} \times$$

$$\times \frac{(\pm)\, 2m_J + 1}{(2J+3)(2J-1)} + \frac{3}{2}\, \frac{d_T}{(2J+3)(2J-1)}\, \delta(m_J', m_J \pm 2)\, \delta(m_I, m_I' \mp 1) \times$$

$$\times\, \delta(m_G', m_G \mp 1) \times \sqrt{I(I+1) - m_I(m_I \mp 1)} \sqrt{G(G+1) - m_G(m_G \mp 1)} \times$$

$$\times \sqrt{(J \pm m_J + 2)(J \pm m_J + 1)(J \mp m_J)(J \mp m_J - 1)},$$

$$< J m_J\, I m_I \mid \mathbf{Q}^{(2)} \cdot \mathbf{V}^{(2)} \mid J' m_J'\, I m_I' > = \sum_F (-)^{3I - 2m_F + F} (2F+1) \times$$

$$\times \{(2J+1)(2J'+1)\}^{\frac{1}{2}} \begin{pmatrix} J & I & F \\ m_J & m_I & -m_F \end{pmatrix} \begin{pmatrix} J' & I & F \\ m_J' & m_I' & -m_F \end{pmatrix} \begin{Bmatrix} J' & I & F \\ I & J & 2 \end{Bmatrix} \begin{pmatrix} J & 2 & J' \\ 0 & 0 & 0 \end{pmatrix} eqQ$$

$$\begin{pmatrix} I & 2 & I \\ -I & 0 & I \end{pmatrix} \frac{}{4}$$

Bak 61 BAKER M R, ANDERSON C H, PINKERTON J, and RAMSEY N F, *Bull Am Phys Soc* **6**, 19 (1961)

Bar 54 BARNES R G, BRAY P J, and RAMSEY N F, *Phys Rev* **94**, 893 (1954)

Ben 55 BENNEWITZ H G, PAUL W, and SCHLIER C, *Z Phys* **141**, 6 (1955)

Ben 63 BENEDICT W S, and HERMAN R, *J Quant Spectrosc Radiat Transfer* **3**, 265 (1963)

Ben 69 BENDER C F, and DAVIDSON E R, *Phys Rev*, **183**, 23 (1969)

Ber 66 BERENDTS B TH, *Thesis* (1966), Nijmegen, The Netherlands

Ber 68 BERENDTS B TH, and DYMANUS A, *J Chem Phys* **49**, 2632 (1968)

Blu 68 BLUYSSEN H, *Thesis* (1968), Nijmegen, The Netherlands

Bri 66 BRIDGE N J, and BUCKINGHAM A D, *Proc Roy Soc* **A295**, 334 (1966)

Buc 68 BUCKINGHAM A D, DISCH R L, and DUNMUR D A, *J Am Chem Soc* **90**, 3104 (1968)

Bur 58 BURRUS C A, *J Chem Phys* **28**, 427 (1958)

Cad 66 CADE P E, and HUO W M, *J Chem Phys* **45**, 1063 (1966)

Cad 67a CADE P E, and HUO W M, *J Chem Phys* **47**, 614 (1967)

Cad 67b CADE P E, and HUO W M, *J Chem Phys* **47**, 648 (1967)

Ced 64 CEDERBERG J W, ANDERSON C H, and RAMSEY N F, *Phys Rev* **136**, A960 (1964)

Dew 66 DEW G D, *J Sci Instr* **43**, 809 (1966)

Dijk 70 DIJK F A VAN, and DYMANUS A, *Chem Phys Letters* **5**, 387 (1970)

Dijk 70a DIJK F A VAN, and DYMANUS A, *Chem Phys Letters* **2**, 235 (1970)

Dre 61 DRECHSLER W, and GRAFF G, *Z Phys* **163**, 165 (1961)

Dym 66 DYMANUS A, *Monograph* No 1 (1966), Atomic and Molecular Research Group, Katholieke Universiteit, Nijmegen, The Netherlands

Edm 60 EDMONDS A R, '*Angular Momentum in Quantum Mechanis*', Princeton University Press, Princeton, New Jersey (1960)

Eve 69 EVERDY J J, *Quarterly Report* No **24** (1969), Atomic and Molecular Research Group, Katholieke Universiteit, Nijmegen, The Netherlands

Fey 68 FEYEN H, *Quarterly Report* No **19** (1968), Atomic and Molecular Research Group, Katholieke Universiteit, Nijmegen, The Netherlands

Fey 68a FEYEN H, *ibid* No **20** (1968)

Fly 64 FLYGARE W H, *J Chem Phys* **41**, 793 (1964)

Fly 68 FLYGARE W H, and GOODISMAN J, *J Chem Phys* **49**, 3122 (1968)

Fly 69 FLYGARE W H, HUTTNER W, SHOEMAKER R L, and FOSTER P D, *J Chem Phys* **50**, 1714 (1969)

Fly 71 FLYGARE W H, BENSON R C, *J Mol Spectr* **20**, 22 (1971)

Ful 65 FULLER G H, and COHEN V W, '*Nuclear Moments*, Appendix I to Nuclear Data Sheets', issued May (1965)

Gor 55 GORDON J P, ZEIGER H J, and TOWNES C H, *Phys Rev* **99**, 1264 (1955)

Gra 63 GRAFF G, and RUNOLFSSON O, *Z Phys* **176**, 90 (1963)

Gra 67 GRAFF G, SCHONWASSER R, and TONUTTI M, *Z Phys* **199**, 157 (1967)

Gun 54 GUNTHER-MOHR G R, TOWNES C H, and VAN VLECK J H, *Phys Rev* **94**, 1191 (1954)

Hel 70 HELMINGER P, LUCIA F C DE, and GORDY W, *Phys Rev Letters* **25**, 1397 (1970)

Heu 68 HEUVEL J, *Monograph* No 7 (1968), Atomic and Molecular Research Group, Katholieke Universiteit, Nijmegen, The Netherlands

Hin 68 HINDERMAN D K, and CORNWELL C D, *J Chem Phys* **48**, 4148 (1968)

Hui 66 HUISZOON C, *Thesis* (1966), Nijmegen, The Netherlands

Hüt 67 HÜTTNER W., and FLYGARE W. H., *J. Chem. Phys.* **50**, 2863 (1967).

Jud 63 JUDD B. R., '*Operator Techniques in Atomic Spectroscopy*', McGraw Hill Book Company Inc., New York (1963).

Kai 70 KAISER E. W., *J. Chem. Phys.* **53**, 1686 (1970).

Kel 39 KELLOGG J. M. B., RABI I. I., RAMSEY N. F., and ZACHARIAS J. R., *Phys. Rev.* **56**, 728 (1939).

Kol 67 KOLOS W., and WOLNIEWICZ L., *J. Chem. Phys.* **46**, 1426 (1967).

Lam 41 LAMB W. E., *Phys. Rev.* **60**, 817 (1941).

Lee 66 LEEUW F. H. DE, *Monograph* No. **3** (1966), Atomic and Molecular Research Group, Katholieke Universiteit, Nijmegen, The Netherlands.

Lee 67 LEEUW F. H. DE, *Quarterly Report* No. **15** (1967), Atomic and Molecular Research Group, Katholieke Universiteit, Nijmegen, The Netherlands.

Lee 67a LEEUW F. H. DE, *ibid.* No. **16** (1967).

Lee 68a LEEUW F. H. DE, *ibid.* No. **18** (1968).

Lee 68b LEEUW F. H. DE, *ibid.* No. **19** (1968).

Lee 69a LEEUW F. H. DE, and MEERTS W. L., *ibid.* No. **23** (1969).

Lee 69b LEEUW F. H. DE, *ibid.* No. **24** (1969).

Lee 69c LEEUW F. H. DE, *ibid.* No. **25** (1969).

Lee 69d LEEUW F. H. DE, and EVERDY J. J., *ibid.* No. **25** (1969).

Lee 69e LEEUW F. H. DE, and DYMANUS A., *J. Chem. Phys.* **50**, 1393 (1969).

Lee 70a LEEUW F. H. DE, and DYMANUS A., *Chem. Phys. Letters* **7**, 288 (1970).

Lee 70b LEEUW F. H. DE, *Quarterly Report* No. **28** (1970), Atomic and Molecular Research Group, Katholieke Universiteit, Nijmegen, The Netherlands.

Lee 70c LEEUW F. H. DE, *ibid.* No. **29** (1970).

Lip 66 LIPSCOMB W. N., in: '*Advances in Magnetic resonance*', Vol. **2**, ed. J. S. Waugh, Academic Press, New York (1966).

Mar 57 MARSHALL S. A., and WEBER J., *Phys. Rev.* **105**, 1502 (1957).

Mat 65 MATTAUCH J. H. E., THIELE W., and WAPSTRA A. H., *Nucl. Phys.* **67**, 1 (1965).

McL 67 MCLEAN A. D., and YOSIMINE M., *J. Chem. Phys.* **47**, 3256 (1967).

Mee 69 MEERTS W. L., *Quarterly Report* No. **25** (1969), Atomic and Molecular Research Group, Katholieke Universiteit, Nijmegen, The Netherlands.

Mes 62 MESSIAH A., '*Quantum Mechanics*', North-holland Publishing Company, Amsterdam (1962).

Mor 67 MORINO Y., and MATSUMURA C., *Bull. Chem. Soc. Japan* **40**, 1095 (1967).

Mue 68 MUENTER J. S., *J. Chem. Phys.* **48**, 4544 (1968).

Mue 70 MUENTER J. S., AND KLEMPERER W., *J. Chem. Phys.* **52**, 6033 (1970).

Mur 68 MURPHY J. S., and BOGGS J. E., *J. Chem. Phys.* **49**, 3333 (1968).

Qui 58 QUINN W. E., BAKER L. M., LA TOURRETTE J. T., and RAMSEY N. F., *Phys. Rev.* **112**, 1929 (1958).

Rab 39 RABI I. I., MILLMAN S., KUSCH P., and ZACHARIAS J. R., *Phys. Rev.* **55**, 526 (1939).

Ram 40 RAMSEY N. F., *Phys. Rev.* **58**, 226 (1940).

Ram 50 RAMSEY N. F., *Phys. Rev.* **78**, 221 (1950).

Ram 50a RAMSEY N. F., *Phys. Rev.* **78**, 699 (1950).

Ram 51 RAMSEY N. F., *Phys. Rev.* **83**, 540 (1951).

Ram 53 RAMSEY N. F., *Phys. Rev.* **91**, 303 (1953).

Ram 56 RAMSEY N. F., '*Molecular Beams*', Oxford University Press, London (1956).

Ran 65 RANK D. H., RAO B. S., and WIGGINS T. A., *J. Mol. Spectr.* **17**, 122 (1965).

Rot 70 ROTHENBERG S., YOUNG R. H., and SCHAEFER III H. F., *J. Am. Chem. Soc.* **92**, 3243 (1970).

Sch 57 SCHLIER C., *Z. Phys.* **147**, 600 (1957).

Sch 61 SCHLIER C., *Fortschritte Phys.* **9**, 455 (1961).

Sch 70 SCHARPEN L., MUENTER J. S., LAURIE V. W., *J. Chem. Phys.* **53**, 2513 (1970).

Ste 64 STEVENS R M, and LIPSCOMB W N, *J Chem Phys* **41**, 184 (1964)

Taf 68 TAFT H, and DAILY B P, *J Chem Phys* **48**, 597 (1968)

Tay 69 TAYLOR B N, PARKER W H, and LANGENBERG D N, *Rev Mod Phys* **41**, 375 (1969)

Tha 64 THADDEUS P, KRISHER L, and LOUBSER J, *J Chem Phys* **40**, 257 (1964)

Tow 55 TOWNES C H, and SCHAWLOW A L, '*Microwave Spectroscopy*', McGraw Hill Book Company Inc, New York (1955)

Tow 55a TOWNES C H, DOUSMANIS G, WHITE R, and SCHWARTZ R, *Disc Far Soc* **19**, 556 (1955)

Ver 69 VERHOEVEN J A TH, *Thesis* (1969), Nijmegen, The Netherlands

Vle 32 VLECK J H VAN, '*Electric and magnetic Susceptibilities*', Oxford University Press, Oxford, England (1932)

Wac 67 WACHEM R VAN, *Thesis* (1967), Nijmegen, The Netherlands

Web 68 WEBB D U, and RAO K N, *J Mol Spectr* **28**, 12 (1968)

Wei 63 WEISS R, *Phys Rev* **131**, 659 (1963)

Whi 55 WHITE R L, *Rev Mod Phys* **27**, 276 (1955)

Wic 48 WICK G C, *Phys Rev* **73**, 51 (1948)

Woł 66 WOLNIEWICZ L, *J Chem Phys* **45**, 515 (1966)

Yut 62 YUTSIS A, LEVINSON I, and VANAGAS V, '*The Theory of Angular Momentum*', Israel Program for Scientific Translations, Jerusalem (1962)

SAMENVATTING

In dit proefschrift worden elektrische en magnetische eigenschappen van de molekulen HF, HCl en OCS experimenteel bepaald uit metingen verricht met een molekulaire bundel elektrische resonantie (MBER) spektrometer.

De spektrometer (Hoofdstuk 2) is gebouwd volgens principes gebruikt door Drechsler en Gräff (1961), Weiss (1963) en Van Wachem (1967). Het kombineren van de eigenschappen van hun apparatuur in een enkel apparaat (homogeen magneetveld in resonantiegebied en universele detektor), het optimaliseren van de instrumentele kondities en het gebruikmaken van vierpoolvelden die geschikt zijn voor hoge spanningen, maakten de in dit proefschrift beschreven experimenten mogelijk.

De theorie van de spektra (Hoofdstuk 3) is gelijk aan die gebruikt door Ramsey en zijn medewerkers in hun onderzoekingen aan het waterstofmolekuul. Volgens deze theorie worden de posities van de resonantielijnen in de spektra uitgedrukt in termen van koppelingskonstanten. De koppelingskonstanten in dit onderzoek zijn: het elektrische dipoolmoment, de kern hyperfijn koppelingskonstanten, het molekulaire magnetische moment, de anisotropie in de magnetische susceptibiliteit en de anisotropie in de magnetische afscherming van de kernen. De laatste drie typen koppelingskonstanten zijn moeilijk te meten vanwege het kleine effekt dat ze hebben op de spektra en waren voor het HF en HCl molekuul tot nu toe nog niet bepaald. De bepaling hiervan vormt het hoofdonderwerp van dit proefschrift. De metingen aan OCS hebben voornamelijk gediend om de apparatuur te testen, doch hebben ook duidelijkheid gebracht in dubbelzinnige resultaten verkregen uit eerdere onderzoekingen.

De gemeten spektra en de resultaten voor de koppelingskonstanten zijn gegeven in hoofdstuk 4.

Hoofdstuk 5 is gewijd aan de interpretatie en de diskussie van de verkregen resultaten. De invloed van de molekulaire vibraties op de analyses van de koppelingskonstanten is niet verwaarloosbaar (enige procenten) en is zo goed als mogelijk meegenomen. De volgende grootheden konden uit de gemeten koppelingskonstanten berekend worden: de anisotropie in de diamagnetische susceptibiliteit, het molekulaire kwadrupoolmoment, en de anisotropie in de diamagnetische afscherming van de kernen. De laatste drie grootheden waren eveneens voor het HF en HCl molekuul nog niet eerder bepaald.

Het elektrische dipoolmoment van OCS is bepaald met een nauwkeurigheid van 4×10^{-5}, terwijl het magnetische moment van HCl bepaald is tot op 6×10^{-5}. De molekulaire kwadrupoolmomenten zijn bepaald met een nauw-

keurigheid van een paar procent en de anisotropiën in de diamagnetische afscherming van de waterstofkernen in HF en HCl zijn bepaald binnen 10 %.

De verkregen resultaten zijn vergeleken met resultaten, indien aanwezig, van andere onderzoekers en met resultaten van ab-initio berekeningen. De resultaten voor de reeds eerder gemeten koppelingskonstanten zijn in zeer goede overeenstemming met resultaten uit vroegere onderzoekingen. Zeer goede overeenstemming is ook gevonden tussen het experimenteel bepaalde molekulaire kwadrupoolmoment van HF en het resultaat van een recente theoretische berekening (Bender en Davidson (1969)). In het geval van HCl is de overeenstemming wat minder goed. Dit is voornamelijk te wijten aan het feit dat voor het HCl molekuul de berekeningen ingewikkelder zijn vanwege het grotere aantal elektronen. De gemeten diamagnetische anisotropiën van de waterstofkernen in HF en HCl konden niet vergeleken worden met theoretische waarden, daar van deze grootheden geen berekeningen bestaan.

De konklusies van dit proefschrift zijn dat elektrische en magnetische eigenschappen van de molekulen HF, HCl en OCS nauwkeurig bepaald kunnen worden met een MBER spektrometer. Voor het HF molekuul zijn nauwkeurige ab-initio berekeningen mogelijk. De voor het HCl bestaande berekeningen verklaren de gemeten grootheden nog onvoldoende. Het verdient aanbeveling om de invloed van de molekulaire vibraties in de theoretische berekeningen mede te nemen.

STELLINGEN

I

Uit de in dit proefschrift beschreven metingen aan HF en HCl en analoge metingen aan DF en DCl kan het molekulaire quadrupool moment bij evenwichtsafstand van de kernen bepaald worden.

II

Voor sommige molekulen is het mogelijk om de verhouding van het magnetische moment van het molekuul en het magnetische moment van een van de kernen in het molekuul zeer nauwkeurig te meten. Dit biedt een uitstekende mogelijkheid om een ijkschaal van molekulaire magnetische momenten vast te leggen.

III

In de door Bakker, van Kempen en Wyder aangegeven methode voor de bepaling van temperaturen in het gebied van 0.2-1° K zijn resultaten van de BCS theorie gebruikt die niet van toepassing zijn op het door hen onderzochte systeem.

J. W. M. BAKKER, H. VAN KEMPEN en P. WYDER, *Phys. Letters* **31A**, 290 (1970).
J. W. M. BAKKER, H. VAN KEMPEN en P. WYDER, *Proc. of the Third International Cryogenic Engineering Conference*, Berlijn (1970), p. 217.

IV

Eisberg en Ziock geven een verkeerde interpretatie van het theorema van Unsöld.

UNSÖLD, *Ann. d. Physik* **82**, 379 (1927).
R. M. EISBERG, '*Fundamentals of Modern Physics*', John Wiley & Sons, Inc., New York (1961), p. 312.
K. ZIOCK, '*Basic Quantum Mechanics*', John Wiley & Sons, Inc., New York (1969), p. 98.

V

De bepaling van elektronendichtheden in plasma's met de mikrogolf trilholte methode is niet zinvol bij frequenties veel lager dan de plasmafrequentie. Dit in tegenstelling tot de bewering van Burke en Crawford.

B. E. BURKE and F. W. CRAWFORD, *Am. J. Phys.* **32,** 942 (1964).

VI

In het door Neumann uitgevoerde MBER experiment aan het open schil molekuul NO zijn zodanige overgangen gemeten dat een test van de gebruikte Hamiltoniaan niet mogelijk is.

R. M. NEUMANN, *Astrophys. J.* **161,** 779 (1970).

VII

De voor het HCl molekuul optredende ongeldigheid van de Born-Oppenheimer approximatie, zoals voorgesteld door Kaiser in zijn behandeling van het elektrisch dipool moment van dit molekuul, was misschien niet gevonden als bij de analyse van de experimentele resultaten voldoende rekening was gehouden met de invloed van de vibraties van het molekuul.

E. W. KAISER, *J. Chem. Phys.* **53,** 1686 (1970).

VIII

De in dit proefschrift gegeven formule 3.11 wordt in vele quantum mechanica leerboeken ten onrechte afgedaan als een wiskundig tussenresultaat voor de berekening van overgangswaarschijnlijkheden.

IX

Het door de „commissie modernisering leerplan natuurkunde" voorgestelde leerplan voor de bovenbouw V.W.O. waarbij naast een voor allen vereiste kernleerstof, te doceren tot en met de voorlaatste klas, een drietal keuze onderwerpen behandeld wordt zal meer stimulerend werken op de belangstelling voor dit vak.

Commissie Modernisering Leerplan Natuurkunde, *Interimrapport*, V.W.O. – bovenbouw, oktober 1969.

X

Bij het naderen van voorsorteerstroken dienen de positioneringen van deze stroken en de daarmee samenhangende richting aanduidingen voldoende vroeg van te voren en op een duidelijke wijze aangegeven te zijn.

25 juni 1971

F. H. DE LEEUW.